A COMPUTER MODEL OF THE POLAR F-REGION IONOSPHERE

A

DISSERTATION

Presented to the Faculty of the

University of Alaska in Partial Fulfillment

of the Requirements

for the Degree of

DOCTOR OF PHILOSOPHY

By

Brenton John Watkins B.Sc., M.Sc.

Fairbanks, Alaska

May 1976

A COMPUTER MODEL OF THE POLAR F-REGION IONOSPHERE

RECOMMENDED:

Daniel W. Swift

W. M. Sackinger

Robert S. Wainwright

Thom D. Bates

Hilbert F. Belon

Chairman, Advisory Committee

APPROVED:

K. B. Chaffee
Director, Geophysical Institute

Febr. 21, 1976
Date

Vice President for Research

21 Apr. 1976
Date

ABSTRACT

A numerical computer model of the geomagnetically quiet, high latitude F-region ionosphere has been constructed. A mathematical model of the steady state polar convective electric field pattern is used in conjunction with the production and loss processes (viz., photoionization, auroral particle precipitation, chemical recombination and polar wind loss). The continuity equation is solved for the ionization density as a unit volume moves across the polar cap and through the auroral zones. The problem is worked with as realistic a geometry as possible to incorporate the effects of the separation of the geographic pole and invariant pole: This is necessary to evaluate the universal time dependence of the ionosphere.

Contours of peak electron density are computed for various geophysical conditions. Results show small but significant changes in the F-region morphology within the polar cap in response to varying the asymmetry of the global convective electric fields; no corresponding change was noted in the morphology of the mid-latitude ionospheric trough. The universal time response of the ionosphere produces large diurnal changes in both the polar cap densities and trough morphology. In agreement with observations, the model shows diurnal variations of the polar cap density by a factor of about 10 at midwinter and a negligible diurnal

variation at midsummer. The phase of the polar cap diurnal variation is such that the maximum density occurs approximately when the geomagnetic pole is nearest to the sun (i.e. when the polar cap photoionization is a maximum).

The minimum density of the trough has no significant diurnal variation, but the longitudinal extent of the trough does have a marked diurnal variation.

Within the accuracy of this model, the results suggest that the transport of ionization from the dayside of the auroral zone can numerically account for the maintenance of the polar cap ionosphere during winter when no other sources of ionization are present.

There is little seasonal variation in the depth or latitude of the ionization trough, the predominant seasonal change being the longitudinal extent of the trough.

The polar wind loss of ionization is of secondary importance compared to chemical recombination. An equilibrium calculation of the quantity of vibrationally excited N_2 in the auroral oval indicates this species to be unimportant in affecting recombination. Also, the velocity dependence of the reaction $O^+ + N_2 \rightarrow NO^+ + N$ is not important in affecting recombination during quiet conditions when the ion-neutral relative velocity is small.

TABLE OF CONTENTS

LIST OF FIGURES

ACKNOWLEDGEMENTS

The research in this dissertation was financially supported in part by the National Science Foundation Grant 27640, and in part by State of Alaska funds.

Thanks are due to members of my advisory committee, Professors H. F. Bates, A. E. Belon, R. D. Hunsucker and D. W. Swift for help and advice both before and during my thesis work. Each has contributed in their own way to the completion of this thesis.

Many other members of the Geophysical Institute have aided me through useful discussions. For these invaluable talks I thank Prof. S. -I. Akasofu, Henry Cole, Prof. V. Degen, Prof. Sivjee, Dr. A. T. Y. Lui, Prof. M. H. Rees, and Dr. F. Yasuhara.

An outstanding debt of gratitude is owed to Prof. R. Parthasarathy, whose door was always open for countless scientific discussions. These interactions have contributed greatly to my eduction and will prove beneficial to me, long after this thesis is forgotten.

I appreciate help with the computing that has been given to me by Tom Wetmore, Shirley Liss, and Max Buhler.

Most of the long and tedious typing task was performed by Mrs. Sandi Moseley. I thank her for persevering with this demanding task.

Finally I thank my wife Helen for aid with the drafting and company through all the frustrations of the Alaskan life.

CHAPTER I

INTRODUCTION AND NATURE OF THE PROBLEM

The objective of this thesis is to further the understanding of the polar F-region ionosphere. The inspiration for this work was derived from observations of electron density profiles in the auroral zone by the incoherent scatter radar at Chatanika, Alaska.

A numerical computer model has been developed to simulate the ionosphere by solving the time-dependent equation of continuity for ionization over the entire polar ionosphere. Such a model then allows an understanding of the global morphology of the ionosphere and leads to an easier understanding of single point observations.

A large scale ionosphere model is desirable because of the occurrence of horizontal plasma velocities up to several hundred meters per second. The time constant for ionization loss is over an hour, and in this time plasma can be transported large distances. The result is that it is often impossible to understand a single point observation of an electron density profile because it is necessary to know the previous temporal history (for about an hour) of the production and loss processes within the measured volume of plasma.

This problem is linked with the problem of the ionization troughs at auroral latitudes. The morphology of these troughs on a large scale should result from the computer model.

For simplicity attention will be confined to conditions of low sunspot number and quiet geomagnetic activity in the high latitude region outside the plasmasphere. The geophysical conditions used in this work correspond to relatively low particle precipitation

and to maximum electric field magnitudes of 20-30 mV/m in the polar cap and auroral zones. In addition a small sized auroral oval and convective electric field region is assumed (presented in Chapter IV).

For a general introduction it is of value to examine some data to illustrate the nature of the problem. Figure 1.1 shows electron density and ion velocity data from the Chatanika incoherent scatter radar for a summer period of 24 hours. Note that in conjunction with the horizontal ion velocities, there are fairly rapid variations in the electron density at different altitudes. To understand such behavior in the electron density data it is necessary to know where the plasma came from before the time of measurement - for example it may have recently traversed a region of high ionization production such as an aurora so that an anomalously high density is recorded. Hence, without all the information on auroral positions, global electric fields, etc., we cannot necessarily explain in detail any given data such as Figure 1.1. By reversing the problem and stating the geophysical conditions, we can learn what kinds of electron density morphology are compatible with what kinds of conditions.

In summary, the following topics are investigated with the computer model:

1.) The morphology of the polar F-region ionosphere and its seasonal changes.

2.) The universal-time dependence of the ionization trough morphology. This point has not been explicitly mentioned in the literature in relation to trough morphology but is

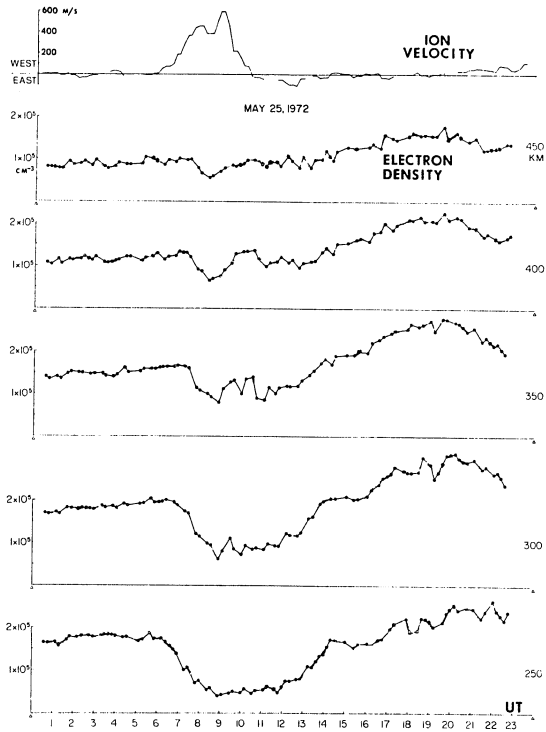

Figure 1.1 Density and velocity data for the day of May 25, 1972 from the Chatanika incoherent scatter radar.

proposed to exist on the basis that the geographic and geomagnetic poles are separated. This ionization trough (or main trough) has been studied in past by ground based ionosondes (eg. Stanley 1966, Wagner et al, 1973), airborne ionosondes (Wagner et al, 1973), satellite-borne ionosondes (eg. Muldrew, 1965) and satellite particle detection (eg. Tulunay and Sayers, 1971) as well as incoherent scatter radars.

3.) The effects of a changing polar electric field configuration which are associated with interplanetary field changes.

The continuity equation to be solved is of the form,

$$\frac{Dn}{Dt} = \frac{\partial n}{\partial t} + \vec{v}_{\perp}\cdot\nabla n = q - l - \nabla\cdot(n\vec{v}_{\parallel}) - n\nabla\cdot\vec{v}_{\perp}$$

where $\frac{Dn}{Dt} = \frac{\partial n}{\partial t} + \vec{v}_{\perp}\cdot\nabla n$ is the rate of change of electron density n in a unit volume as it moves horizontally with velocity $\vec{v}_{\perp}$ (the $\vec{E} \times \vec{B}$ drift velocity). The photoionization or auroral ionization production rate is given by q, and l denotes the chemical recombination rate. The term containing $\vec{v}_{\parallel}$, the velocity parallel to the B field is generally not numerically large compared to other terms. At high latitudes it is normally composed of field aligned diffusion of ionization called the polar wind; however this can also be affected by field aligned neutral gas motions (see Chapter V). The polar wind has been retained in this work; however, in Chapter III it is shown that omitting it results in only a few per cent difference. The final term vanishes because the $\vec{E} \times \vec{B}$ drift is incompressible.

Briefly, the objective is to obtain electron density contours over the previously defined polar region. This will be done by first defining a mathematical model to simulate the plasma motions. Next, focusing on a unit volume of plasma, its density will be computed as the volume moves in small steps along the path. At each of these steps the continuity equation will be solved. By similarly following many plasma paths, density values are calculated at many locations; this then permits contours to be drawn. The method has the advantage that horizontal transport into the measuremert volume is transformed away. The contribution to ionization production from auroral ionization orginates from an assumed auroral oval location based on observations (for Q=1 conditions). The solar photoionization is computed for any given location by first calculating the solar zenith angle for the particular time, day, and location.

It will be shown that the polar wind is not as important as chemical recombination in causing ionization loss. This recombination rate may be increased by the presence of vibrationally excited nitrogen or increased ion-neutral relative velocity. However, these will be demonstrated to be unimportant for solving this particular problem.

In all that follows we will be referring to the F region of the ionosphere, i.e. the 150-600 km region. Since the peak ionization occurs around 300 km, the problem will be further restricted to the 200-400 km altitude range as we will be mainly interested in the peak ionization densities.

The morphology and interaction of auroral oval with the magnetosphere, as outlined for example by Akasofu (1968), is assumed in this thesis.

CHAPTER II

IONIZATION PRODUCTION PROCESSES

There are only two sources of ionization in the high latitude ionosphere; photoionization, and ionization produced by precipitating particles, the latter process being insignificant at lower latitudes. A computer program has been developed to calculate photoionization rates from 200-400 km altitude, and precipitating auroral ionization obtained from an assumed auroral oval.

2.1 Photoionization

Solar radiation of wavelengths less than about 900 A is responsible for the production of ionization in the ionosphere (Whitten and Poppoff, 1971). This radiation enters the top of the ionosphere and ionizes the neutral constituents, the maximum production rate for overhead sun occurring at an altitude of about 140 km (Hinteregger, et al, 1965).

To compute the photoionization rate at a particular altitude, we must know the solar flux at that altitude after it has traversed the overlaying portion of the upper ionosphere. The ionization production rate then depends on the neutral gas density and the ionization cross-section.

Although O^+, O_2^+, and N_2^+ ions are all formed in the F region, the primary production rate of O^+ (about 2×10^2 cm^{-3} at 300 km for overhead sun) is at least an order of magnitude greater than other ions (Hinteregger et al, 1965). This is because atomic oxygen is the dominant neutral species, the ionization potentials are all of similar values (12 - 15 ev) so differences in ionization potential have little effect.

For an overhead sun, the solar flux F at an altitude z is given by $F=F_o e^{-\tau}$ where F_o is the flux at the top of the atmosphere and τ is the optical depth. The optical depth refers to the vertical distance for the flux to decrease by a factor e.

$$\tau = \int_z^\infty n\,\sigma\,ds$$

where n = neutral number density

σ = absorption cross-section

This expression can be rewritten in terms of the scale height (H = kT/mg) at the point of interest to produce a simpler formulation (eg. Banks and Kockarts, 1973) as,

$$\tau = n\,H\,\sigma$$

When the solar zenith angle is large the solar flux must traverse more of the neutral atmosphere before arriving at the measurement point; thus the integral along the path length is larger.

For the general case of incoming radiation at any solar zenith angle χ, including angles near 90°, Chapman (1931) derived the "Chapman Function" $Ch(\chi)$ for spherical geometry. The optical path is $Ch(\chi)\tau$. Thus the optical depth is given by

$$\tau = n\,H\,\sigma\,Ch(\chi)$$

The flux arriving at an altitude is then simply obtained from the above mentioned expression, viz.,

$$F = F_o\, e^{-\tau}.$$

A slight modification to the Chapman Function was made by Green et al. (1964), Fitzmaurice (1964), and Swider and Gardener (1969). These

authors did not assume a constant scale height atmosphere. In place of the Chapman Function they introduced the function G derived from spherical geometry. Their results are summarized as follows:

For $\chi < (\pi/2)$

$$\tau(X,\chi) = n\, H\, \sigma\, G(X,\chi) \qquad (1a)$$

where $X = (Re + z)/H$

H = local scale height of neutral gas

Re = earth's radius

$$G(X,\chi) = \exp\left[(\chi^2/2) / (1 - 0.115\chi^2 - 2\chi^4)\right]$$

$$\alpha = \frac{1 - 0.115(\pi/2)^2 - [0.5(\pi/2)^2] / [\ln(\pi/2X)^{1/2}]}{(\pi/2)^4}$$

For $\chi > (\pi/2)$

$$\tau(X,\chi) = n(a)\, H(a)\, G(Y,\chi) \qquad (1b)$$

where $n(a)$ = number density as above but evaluated at the minimum height (a) of the solar flux before it reaches the observation point, and is simply calculated geometrically

$H(a)$ = scale height at height a

$$G(Y,\chi) = (\pi Y/2)^{1/2}[1 + \mathrm{erf}\{-\cot\chi\,(Y/2)^{1/2}\}]$$

$$Y = (Re + a)/H$$

The photoionization was calculated using (1a,b).

As the next step, photoionization rates can now be computed (eg. Whitten and Poppoff, 1971) from,

$$\frac{d[O^+]}{dt} = \int_0^\lambda F(\lambda)[O]\,\sigma(\lambda)\,d\lambda$$

where $d[O^+]/dt$ is the production rate of O^+ ions, $F(\lambda)$ is the flux at the wavelength λ, $[O]$ is the number density of atomic oxygen, and $\sigma(\lambda)$ is the wavelength dependent ionization cross-section.

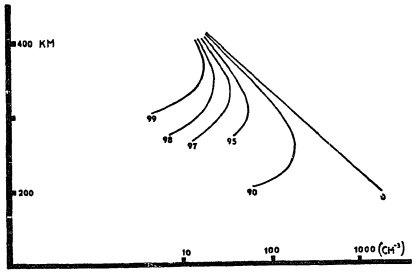

Figure 2.1 A plot of photo ionization rate (0-1000 cm^{-3}) vs altitude (0-400 km) for some selected solar zenith angles (0-99 degrees).

This thesis uses the atmospheric model of Banks and Kockarts (1973), and since these authors have already computed the photoionization rate for low sunspot number and overhead sun, it has been simpler to adopt their values. Then using the previous mentioned theory, the values are modified for various solar zenith angle using equation (1a,b).

From the overhead-sun production rate, and using the above functions to calculate the optical depths, the ionization production rate for any solar zenith angle can be computed.

The computer program for this task reads and stores a neutral density model; then given a solar zenith angle, it produces values of photoionization rate for differing heights. Some sample computations are shown in Figure 2.1.

2.2 Auroral Particle Precipitation as a Source of Ionization for the Polar F-Region Ionosphere

In this section we wish to estimate the production of ionization caused by precipitating particles in the auroral oval. Since there is such a great variety of possible auroral conditions, this work has been limited to modeling the quiet-time auroral oval. These conditions are characterized by a small auroral oval (Q=1), relatively low auroral ionization inputs, and electric field magnitudes no greater than 25 - 30 mv/m. The geometrical aspect will be treated in Chapter IV; this chapter will deal with the ionization inputs only.

A. The Dayside Auroral Oval

The dayside auroral oval is produced by precipitating particles whose energy spectrum is peaked around 100 ev (Heikkila and Winningham, 1971) producing substantial ionization at F-region altitudes

(Rees, 1963). This portion of the auroral oval is often termed the polar cusp region because of the cusp-like geometry of the magnetosphere from which the ionization originates.

Knudsen (1974) estimated the rate of increase of ionization (from satellite measured flux values) for a unit volume as it moves through the dayside auroral oval. His values of 2×10^5 cm^{-3} (around the F-region peak altitude), for a time duration of 5 minutes for a unit volume of plasma to traverse the dayside auroral oval, imply a production rate of 11 ion pairs cm^{-1} sec^{-1}. Similar rates were computed by Banks et al. (1974b) using a polar cusp type input spectrum. These numbers range from 20 cm^{-3} sec^{-1} at 200 km to 4 cm^{-3} sec^{-1} at 380 km, and have been used in this thesis.

It should be stressed that there is some variability in the observed energy and number flux. There is also some uncercainty in the time required for a volume of plasma to traverse the dayside auroral oval. This is because electric field data (and hence the motions of ionization) show very complex behavior in this region (see Chapter IV, Figure 4.2). Heppner (1973) has interpreted the motions as "turbulent".

It is thus likely that we may have underestimated the auroral ionization input through an under-estimate of the time spent by the moving unit volume beneath the precipitation region.

B. The Night-side Auroral Oval

The night-side auroral oval, by comparison with the day-side, is often characterized by precipitating particles of higher energies (up to a few keV). The aurora here can be classified into two

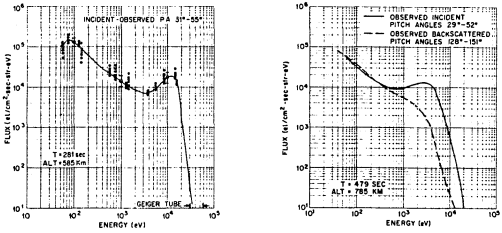

Figure 2.2 Energy-flux data in the F-region ionosphere above discrete and diffuse aurora.
Left: Data taken above bright discrete aurora.
Right: Data taken above nearby diffuse aurora.
(after Reasoner and Chappell, 1973)

types, commonly called discrete and diffuse because of their visual appearance. The difference in energy is shown in Figure 2.2. Although the two types have similar fluxes in the 100 eV energy range (these energies produce most of the F-region ionization, Banks et al., 1974b), there are very marked differences at energies greater than a few keV (these produce ionization much lower in the ionosphere, 100 - 120 km). Other satellite-measured data (eg. Caverly, 1975) show similar spectral differences. We would thus expect little differences in the F-region auroral production rates between discrete and diffuse aurora.

The data of Figure 2.2 were taken from rocket data of Reasoner and Chappell (1973). Banks et al. (1974b) used data from these authors' rocket flight and computed the altitude profile of the ionization rate in the ionosphere for an optically bright discrete auroral arc structure. At F-region altitudes these values are only a factor of 2 - 3 greater than the dayside auroral oval values mentioned earlier.

For simplicity, the values given for the dayside auroral oval have been used on the nightside as well, over a precipitation region shown later in Chapter IV (Figure 4.3).

For the quiet conditions that are applicable in this work, satellite photographs of the auroral oval (Lui et al., 1975) show little or no discrete aurora. Even if the model were expanded to include more disturbed conditions with discrete aurora, inclusion of only the low energy particles would be satisfactory.

A large ionization peak at about 110 km associated with discrete aurora (Hunsucker, 1975) has no effect on the F-region den-

sities (at 300 - 350 km) through diffusion. This is because of the high collision frequency at the lower altitudes which limits upward diffusion. The effect can be evaluated by computing the upward diffusion speed versus the time constant for chemical recombination.

One of the largest auroral E-region peaks (with a very large vertical density gradient) observed by the Chatanika incoherent scatter radar is given in the Figure 11 of the paper by Bates and Hunsucker, (1974). The peak density of 1.3×10^6 cm^{-3} occurred at 110 km altitude and the layer thickness extended from 100 - 140 km. The upward diffusion near the top (125 km) of this layer has been calculated as 20 cm/sec using the expression for diffusion velocity given by Whitten and Poppoff (1971). At these altitudes the recombination lifetime depends on the density, but can vary between 10 - 100 seconds (for densities of $0.5 - 7 \times 10^5$ el cm^{-3}). The vertical distance traveled before recombination is then 20 meters at most.

These diffusion speeds are very small by comparison with possible vertical neutral wind effects. For example, if ionization is slowly diffusing upward through the neutral constituent that has a 25 m/s vertical component (a typical value, see Rieger, 1974), then the vertical distance traveled before recombination would be about 250 meters which is still a negligible distance.

CHAPTER III

IONIZATION LOSS PROCESSES IN THE IONOSPHERE

3.1 Chemical Recombination

The most rapid means of ionization loss in the F region is the removal of O^+ (the dominant ion) by the following two chains of chemical reactions (Whitten and Poppoff, 1971),

$$O^+ + N_2 \rightarrow NO^+ + N \text{---------- (1)}$$

$$O^+ + O_2 \rightarrow O_2^+ + O \text{----------(2)}$$

$$NO^+ + e \rightarrow N + O \text{----------(3)}$$

$$O_2^+ + e \rightarrow O + O \text{----------(4)}$$

Assuming the rate constants for the above reactions are K_3, K_4, α_5, α_2 respectively; the relevant rate equations for quasi-chemical equilibrium are,

$$\frac{d}{dt}[O^+] = \{ K_3 [N_2] + K_4 [O_2] \} [O^+]$$

$$\alpha_2 [O_2^+] N_e = K_4 [O_2] [O^+]$$

$$\alpha_5 [NO^+] N_e = K_3 [N_2] [O^+]$$

The square brackets above denote number densities of the species enclosed and N_e refers to electron number density. Assuming charge neutrality we have,

$$N_e = [O^+] + [NO^+] + [O_2^+]$$

Rearranging the above rate equations and eliminating $[O^+]$ results in,

$$\frac{d}{dt}[O^+] = \frac{(K_3[N_2] + K_4[O_2])\, N_e}{1 + \dfrac{K_4[O_2]}{\alpha_2 N_e} + \dfrac{K_3[N_2]}{\alpha_5 N_e}} \text{----------(5)}$$

This equation (5) has been used in this thesis to evaluate the decay of ionization. Note that this expression is dependent on electron density (Ne) and temperature.

The most recent values for the rate constants (units of $cm^3\ sec^{-1}$) have been obtained as,

$$\alpha_5 = (4.2 \times 10^{-7}) \times \left(\frac{T_e}{300}\right)^{-0.5} \qquad \text{Biondi (1974)}$$

$$\alpha_2 = (2.1 \times 10^{-7}) \times \left(\frac{T_e}{300}\right)^{-0.6} \qquad \text{Biondi (1974)}$$

$$K_4 = (1.3 \times 10^{-12}) \times \left(\frac{T_i}{300}\right)^{1.2} \qquad \text{Bortner et al. (1973)}$$

$$K_3 = (8.0 \times 10^{-14}) \times \left(\frac{T_i}{300}\right)^{2.0} \qquad \text{Bortner et al. (1973)}$$

The rate constants are temperature dependent; however, insertion of approximate values in the denominators of equation (5) using $T_i = 1{,}000$, $T_e = 2{,}000$ °K yields,

$$\frac{d}{dt}[O^+] = \frac{(K_3 [N_e] + K_4 [O_2])\, N_e}{1 + \frac{300}{N_e} + \frac{600}{N_e}} \quad (cm^{-3}\ sec^{-1})$$

$$\simeq (K_3 [N_2] + K_4 [O_2])\, N_e \quad \text{(for values of } N_e \gtrsim 10^4 cm^{-3})$$

$$\equiv \beta N_e$$

Here the value of β is about $2 \times 10^{-4}\ sec^{-1}$ at 300 km using the temperatures above and the neutral density model (1000 °K exosphere temperature) of Banks and Kockarts (1973).

Thus, the electron loss rate β is approximately constant for electron densities greater than about 10^4 cm^{-3}. This is the usual way of expressing the electron loss rate in the literature (eg. Whitten and Poppoff, 1971). It is not satisfactory for this thesis because it allows the ionization to decay to unreasonably low values.

3.2 The Velocity Dependent Ion-neutral Reactions

In section 3.1 above, the four relevant reactions for the chemical recombination of O^+ ions were given. Reaction rates of equations (3) and (4) are rapid compared to (1) and (2) and hence these reactions (1) and (2) which control the rate of formation of NO^+ and O_2^+ also control the rate of electron removal. This statement is of course inherent in the mathematical result that β is approximately independent of the α_2 and α_5 rate constants (for N_e greater than 10^4).

Recent laboratory measurements of the rate constant of equation (1) by McFarland, et al (1974) have indicated that its reaction rate is velocity dependent. This has been further explored by Banks, et al. (1974a) in relation to ionization decay in the polar F region. These authors conclude that when electric fields are present (as they are at high latitudes), the relative motions of the ion and neutral constituents will induce a greater production of NO^+ which will subsequently result in enhanced ionization decay through the rapid reaction (3).

It is the purpose of this section to calculate the effect on the electron loss rate, β, due to this velocity dependence and to show that it is not important for this thesis.

In the reference frame of the neutral gas, Banks et al. (1974)

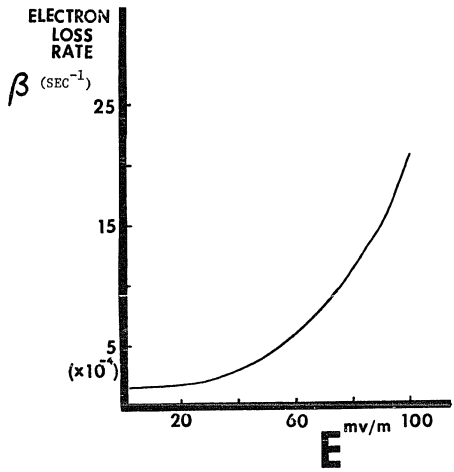

Figure 3.1 Electron loss rate as a function of electric field (measured in the frame of the neutral gas). Values apply for a 1000 degree thermosphere and altitude of 300 km.

infer that an electric field of about 100 mV/m is necessary to produce equal concentrations of O^+ and NO^+ at F-region altitudes. Working further on this subject, Schunk et al. (1975) have discussed the ionospheric effects of reactions (1) and (2) in relation to electric field effects. The electron loss rate, β, has been calculated in this thesis as a function of this effective electric field, using their velocity dependent reaction rates. A sample calculation is shown in Figure 3.1 for a 1000 °K thermosphere and an altitude of 300 km.

It has been assumed here that the polar cap electric fields are no greater than 30 mV/m (see Chapter IV), and since there is evidence that the neutral gas motions are dominated by ion drag (Fedder and Banks, 1972; Nagy et al., 1974; Bates and Roberts, 1976a, 1976b), the effective electric field measured in the neutral gas frame is substantially less (comparisons of ion and neutral velocities in above references indicate the neutral speed is about one half the ion speed). For the problem of interest, only the very lowest portion of the curve of Figure 3.1 is applicable. Hence the velocity dependence of β has been neglected for this study.

3.3 Vibrational Excitation of Nitrogen and Its Effect on Recombination

Referring once again to equations (1) and (4), we focus attention on the most critical reaction controlling the F region, viz. $O^+ + N_2 \rightarrow NO^+ + N$.

Newton et al (1974) suggested that the presence of vibrationally excited nitrogen (N_2^*) in the auroral zone may possibly be important in forming the F-region ionosphere density depressions (troughs).

When the N_2 is in this vibrational excitation state, the above reaction rate is increased (Schmeltekopf et al, 1967, 1968) and O^+ ions dissappear faster.

In this section we wish to estimate the quantity of N_2^* to determine the effectiveness of this species in affecting the recombination rate. From a program of Rees (1975) the production rate of auroral N_2^* has been computed as 17.0 cm^{-3} sec^{-1} at an altitude of 360 km for an electron density of 3.3 x 10^3 cm^{-3}. The program computes the atmospheric effects of an aurora with ionization peak at 110 km, and 5577A emission rate of 4.5 KR in a model atmosphere.

Assuming an atomic oxygen density of 3.9 x 10^8 cm^{-3} at 360 km (obtained from the neutral density model), and the quenching rate of N_2^* with atomic oxygen to be 4.4 x 10^{-14} (Cook et al, 1973), a loss rate can be formulated. Solving for the N_2^* number density by assuming an equilibrium situation (production equals loss) we arrive at the value 1 x 10^6 cm^{-3} which is only 5% of the total N_2 number density at that altitude. A similar calculation at 200 km yields less than 1%.

Returning now to the chemical equation of interest, viz $O^+ + N_2 \rightarrow NO^+ + N$, it is necessary to evaluate the effect (if any) of the above quantities of N_2^* on the electron loss rate β.

For such minor quantities of N_2^* the total effective electron loss rate, β', can be reformulated to include an extra term viz.,

$$\beta' = k_3 [n_2] + k_4 [o_2] + k'_3 [N_2^*] \equiv \beta + \beta_v$$

where

$\beta = \{k_3 [N_2] + k_4 [O_2]\}$ derived previously

$\beta_v = k'_3 [N_2^*]$ is the contribution due to N_2^*

A sample computation (using the rate constant from Schmeltekopf et al, 1968) for 360 km altitude with an ion temperature of 1000°K and a vibrational temperature of 2000°K (a reasonable value, see O'Neil et al (1974) and references therein) yields $\beta \simeq 1.4 \times 10^{-4}$ and $\beta_v \simeq 4 \times 10^{-6}$.

It is concluded that on the basis of the available information, the presence of N_2^* will not significantly affect the electron loss rate in the F region. This is a reasonable conclusion even when allowing for small changes in the neutral density model and laboratory-measured cross-section for N_2^* production. Further, changes in the auroral spectrum to include very bright discrete aurora have little effect on the F-region particle input flux (see Chapter II).

This conclusion is contrary to the suggestion of Schunk and Banks (1975) who invoke equatorward neutral motions to disperse N_2^* and form an electron density trough in the high latitude ionosphere. These authors did not give an estimate of the N_2^* number density.

3.4 The Polar Wind and Its Effect on the Loss of F-Region Ionization

This section deals with one of the important mechanisms affecting both middle and high latitudes. In contrast to the previous sections we are here dealing with ionization loss by vertical diffusion along magnetic field lines, by comparison with chemical reaction discussions that have preceded this section. It is the purpose here to show that this is not as important as chemical recombination in its effect on depleting the F-region ionization.

Although simple arguments have been used by Knudsen (1974) to show that this statement is correct, his logic is misleading and

erroneous even though his conclusion may be correct. He assumed an electron density profile with a corresponding total electron content typical of the dayside of the earth (peak density of 5×10^5 cm^{-3}). Then, taking the polar wind loss rate of Park (1970), he deduced that seven hours were required for the polar wind to deplete the ionosphere. As this time is much greater then the chemical recombination time ($\simeq$ 1.5 hours), he concluded the polar wind was unimportant.

However, this line of argument would be equally valid if we assumed an ionosphere of lower density (eg. $1.5 - 1 \times 10^4$ cm^{-3} peak density) that often occurs in the polar cap or trough region. In such a situation the time to deplete the ionosphere by the polar wind is comparable to chemical recombination times.

The basic problem with these simple arguments is that the polar wind ionization loss is not independent of ionospheric density (Park and Banks, 1975). A more realistic evaluation is thus needed.

Most of the physics of this problem has been well developed, and a review of the basics is contained in Banks (1972) and Park (1973). In brief, H^+ ions may be interchanged between the magnetosphere and ionosphere. At mid-latitudes during the daytime, ionization is transferred from the ionosphere to the plasmasphere, and vice versa at night. The rate of ionization transfer depends on ionospheric densities but ranges typically around 3×10^8 cm^{-2} sec^{-1} at 1000 km altitude. This mechanism appears to be responsible for the maintenance of the mid-latitude ionosphere at night when no other ionization sources are present (Carpenter, 1973). This continual interchange of ionization

is not present at high latitudes because the magnetic field lines, being open, are unable to trap plasma. The polar F-region ionization thus suffers a continuous upward depletion along field lines.

Figure 3.2(a) illustrates the situation. In the region "1" on this figure the dominant ion is O^+. In the region "2" the H^+ ions begin to dominate until an altitude of about 1000 km where O^+ is negligible. In this transition region the accidentally resonant (equal ionization potentials of O and H) reaction $O^+ + H^+ \rightleftarrows H^+ + O$ facilitates such rapid charge exchange that the species are usually considered to be in equilibrium (eg. Banks and Kockarts, 1973). Figure 3.2(b) is extracted from Park and Banks (1975) and shows upward O^+ flux at 500 km plotted against the 500 km O^+ density for the open field line situation of continuous plasma depletion. The 500 km reference altitude used by these authors is quite arbitrary. This relationship in Figure 3.2(b) has been used in the computer program of this thesis to derive an electron loss rate due to the polar wind.

This polar wind loss has been included in all the model calculations presented in later chapters. One calculation was done without this loss and the results are shown in Figure 3.3. The figure shows the density variations as a function of path length for a unit volume of plasma as it moves from the central polar cap to the trough region under the influence of the convective electric field and the varying production and chemical loss rates.

These sample computations point to the polar wind being of secondary importance. However because of the programming ease it has been kept in the model.

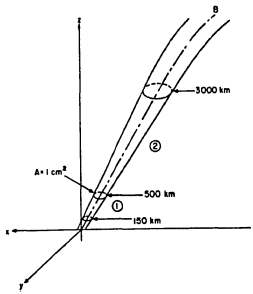

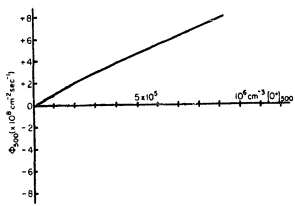

Figure 3.2 An illustration of the magnetic field line geometry and theoretcal polar wind ionization escape flux. Upper diagram,3.2(a),shows the geometry of the magnetic field lines. Lower diagram,3.2(b),a plot of the 500 km upward flux vs density.

(after Park and Banks,1975)

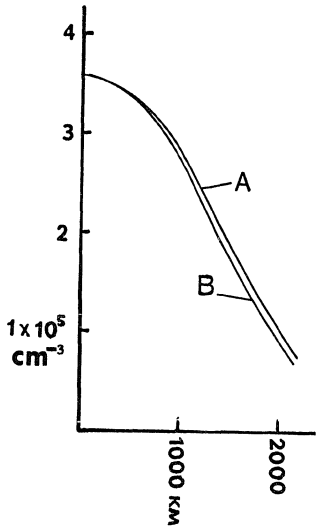

Figure 3.3 Plots of electron density(0--4x10^5 cm^{-3}) vs path length(0--2000 km) for a unit volume as it moves from the central polar cap through the auroral zones.
Curve A is for no polar wind loss of ionization.
Curve B is computed with the polar wind included.

CHAPTER IV

POLAR F-REGION ELECTRIC FIELDS

4.1 Discussion of the Available Data

In this brief discussion of the polar F-region electric fields, emphasis will be placed on the large scale overall picture rather than isolated single point measurements (eg., rocket measurements near auroral arcs, etc). Within this constraint it is found that most of the information now available has been derived from: 1) low altitude polar orbitting satellites equipped with double prove sensors, 2) a statistical buildup of data from many barium releases, and 3) incoherent scatter radar data. Each of these techniques has its own set of advantages and disadvantages. The most relevant data for this study are those from satellites.

In Figure 4.1(a) measurements from satellite traverses of the polar cap in the dawn-dusk meridian are illustrated. These data from Gurnett (1972) are in the form of velocities derived from the electric field data.

A selection of electric field data is shown in Figure 4.1(b) due to Heppner (1972, 1973) who has used similar electric field data to build up a statistical picture of polar ionization motions for low geomagnetic activity. This is shown in Figure 4.2; a double cell pattern is obvious here, with anti-solar-directed flow in the central polar region and return polar-directed flow on either side. The optical auroral oval is located just equatorward of the field reversal region in the area of maximum solar directed velocity (Swift and Gurnett, 1973).

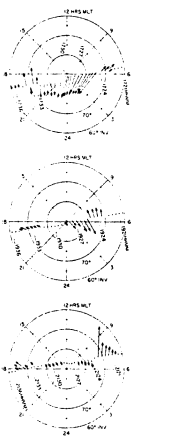

Figure 4.1(a)

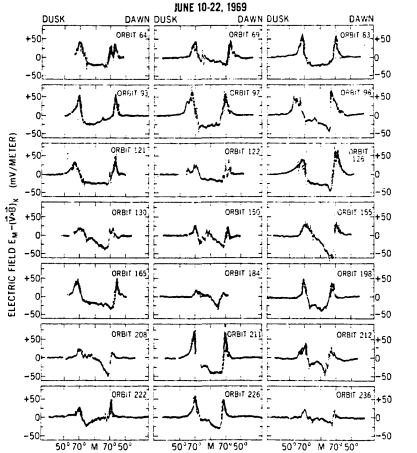

Figure 4.1(b)

Figure 4.1 Sample plots of electric fields and $\vec{E} \times \vec{B}$ plasma drift velocities measured by satellite in the dawn-dusk meridian of the earth. Left figure,4.1(a),plasma velocities. Right figure,4.1(b),the electric field data.

(after Gurnett,1972)

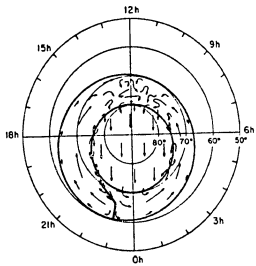

Figure 4.2 A statistical configuration of plasma motions over the polar cap for $K_p \leq 3$ (after Heppner, 1973)

A feature of interest is the symmetry of the anti-solar flow seen in Figure 4.1(b) which can be categorized into three general configurations; viz, a) symmetrical, with a relatively constant $\vec{E} \times \vec{B}$ velocity across the polar cap, b) asymmetrical with a higher velocity on the dusk side, c) asymmetrical with higher velocity on the dawn side. This feature has been studied by Heppner (1972) who found that the asymmetry is associated with the azimuthal component of the interplanetary field. This point was mentioned in Chapter I and is a target of investigation for this thesis as it indicates possible changes in the F-region density morphology. As a note of caution on this latter topic, it should be mentioned that only a single component of electric field is available from these satellite data so that it is possible that the polar cap plasma velocity direction deviates considerably in conjunction with these asymmetric flows. However, statistics seem to indicate primarily an anti-solar direction (Heppner, 1973). Further, the location of the Harang discontinuity may move in longitude depending on the degree of asymmetry, but no such information is available from the literature.

All these satellite data were taken at altitudes around 1000 km, and assuming that the electric fields map to the 300 km level, the resulting $\vec{E} \times \vec{B}$ motion over the polar cap ranges typically from 0.4 to 0.5 km per second. Accepting these velocities and the previously mentioned double cell motion over the polar regions, it has been a necessary task of this thesis to evolve some model for these motions. Such a model allows the ionosphere production and loss processes to be calculated in a parcel of plasma as it moves along a flow stream-

line. The next section of this chapter will discuss the model electric field pattern and its mathematical basis.

4.2 The Electric Field Model

This particular model is the result of the addition of twenty vortex flow patterns. Using the method of images (by analogy with electrostatics), ten vortices and their images in a cylinder have been summed and the resulting flow inside the cylinder has been defined as the required polar ionosphere flow streamlines. Instead of considering the problem in the methodology of fluid mechanics, one can alternatively use the language of electrostatic equipotentials and evolve a velocity through the $\vec{E} \times \vec{B}$ relation, but this is a matter of personal preference.

Figure 4.3 indicates the vortex positions and the resulting flow pattern. The location of auroral particle precipitation is also shown in this figure. There are singularities at the vortex positions; however, these locations are avoidable and in positions of little interest. The number of 20 singularities is fairly arbitrary; this number was decided on because it represented the minimum number to adequately describe the electric field data.

The following is a brief summary of the mathematical basis on which these streamlines were computed. The plasma flow problem is to be solved in the magnetic time-invariant latitude system of the earth, for this is the system in which satellite measurements are ordered and it is these measurements that we wish to simulate. This coordinate system is denoted by the complex z-plane in the model and is the primary frame of reference in which all subsequent computations will take place.

By use of complex variables in the standard fluid mechanics approach using potential theory, one can define a complex potential of a particular fluid flow, the real part of which describes the flow streamlines, and the imaginary part the velocity potential [see for example Robertson (1965) or some other standard text]. A new flow pattern can also be defined by the addition of more than one complex potential, or alternatively if streamlines alone are necessary, summing the stream functions is sufficient.

The complex potential of a single vortex at the position p on the complex plane, with k a constant, is given by,

$$W = i\ k\ \ln\ (z-p)$$

The complex potential for twenty vortices located at positions p_n is given by,

$$W(z) = \sum_{n=1}^{20} i\ k\ \ln(z-p_n)$$

$$= \phi + i\psi$$

The real and imaginary parts above are designated the velocity potential and stream function. A rotation (equivalent to the rotation of the earth) can then be included by adding $\psi^1 = 1/2\ w\ r^2$ to the above stream function, where w is the angular velocity of the earth, r is the distance of the measurement point from the rotation axis with a suitable correction for the curvature of the earth. This rotation has been subtracted from satellite measurements by Heppner (1973) and must be included to obtain the true plasma motions in the magnetic local time-invariant latitude frame of reference.

In summary so far, we have derived a set of streamlines shown

in Figure 4.3 which are to be used for tracing plasma motions over the polar ionosphere. It is necessary to define the speed along each of these lines. Defining this speed is equivalent to defining the constants K_n, and in keeping with the fluid mechanics treatment, the speed can be calculated from,

$$v = W^*(z) = \sum_{n=1}^{20} K_n / r_n$$

where the * denotes complex conjugate and r_n are the distances from the point of measurement to the positions p_n. In Figure 4.3 the speed of flow over the central portion of the figure (equivalent to the polar cap) has been set at about 0.45 km/s to match experimental results.

To simulate asymmetric flow in the polar cap as discussed earlier, the speeds of flow on the various streamlines in the central polar cap have been defined differently. Cross-sections across the dawn-dusk meridian from model calculations are shown in Figure 4.4.

Figure 4.5 illustrates the change when the corotation velocity of the earth is added.

The next chapter will examine in detail how this model was set up for computing the ionosphere electron densities.

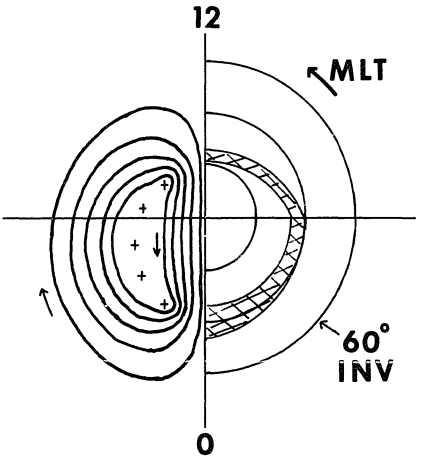

Figure 4.3 The computed plasma flow lines (in the frame of the moving earth). The assumed auroral oval (shaded) is the particle precipitation region used in the computer model.
The crosses denote positions of singularities (see text). The coordinates are magnetic local time and invariant magnetic latitude.

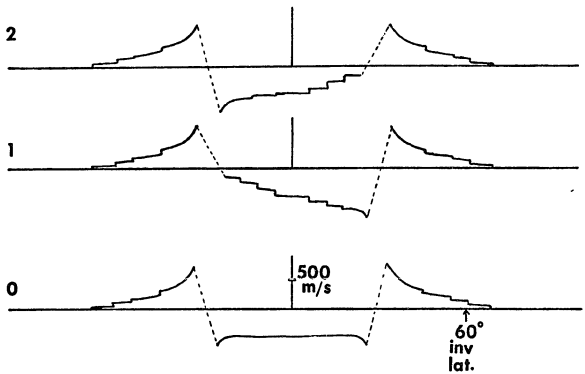

Figure 4.4 Dawn - dusk profiles of plasma velocity derived from the model.

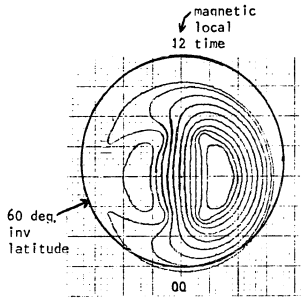

Figure 4.5 A sample computation of the plasma convection of figure 4.3 with the corotation field added. This diagram shows a stagnation point on one side of the earth (left side of figure).

CHAPTER V

NUMERICAL MODELLING OF THE F-REGION IONOSPHERE

5.1 General Procedure

In this chapter the detailed steps and assumptions are discussed that relate to the computer model describing the polar F-region ionosphere.

The electric field model described in the previous chapter has been combined with the various production and loss processes. The general procedure is as follows: Beginning in the central polar cap, an electron density profile is assumed on each of the $\vec{E}x\vec{B}$ flow lines. The computer program then follows each streamline in small steps (90 km apart) computing a new profile at each point and storing each data set on magnetic tape as they are computed. Since the streamlines are closed curves we will eventually end up at the starting position. This computed profile at the end of the closed curve should match the original assumption and this has been achieved by running the program twice to get a self-consistent starting value. The step size of 90 km is arbitrary and represents a compromise between minimizing computer time and maximizing the resolution of the final electron density contours.

Many such streamlines are traced, with the end result that electron density values are computed at many hundreds of points over the polar region. All these data are then plotted and contours are drawn.

5.2 A Detailed Programming Outline

For more detail, the following is a concise outline of the programming functions. The program itself and a flow chart is given in the Appendix.

(1) The electric field problem is set up in the complex plane (as discussed in section 4.2) in preparation for obtaining solutions to the electric field using the method of images.

(2) Other constants for defining the problem are set up in the program. These are: day of year, universal time, and various ephemeris data for computing the solar zenith angle at any given time and geographic position.

(3) The program reads all data cards for the atmospheric model and the transformation from invariant to geographic coordinates.

(4) The type of electric field pattern (see Chapter IV) is set.

(5) Beginning at some arbitrary point on the dawn-dusk meridian the initial electron density profile is assumed. (Any reasonable values can be assumed at first - the correct starting values will be obtained after running the program once). At this point, using the parameters defined in (1) above, plasma speed and a value of the equipotential or stream-function are calculated.

(6) A subprogram is called to find a new point on this same stream-function a fixed distance from the first point.

(7) Using the coordinates of this new point in the invariant latitude-magnetic time coordinate system, transformations are made to the invariant latitude-magnetic longitude system. At this stage after a further transformation to geographic coordinates, the ephemeris data are used in another subprogram to get the photoionization rate. Finally the continuity equation is solved at this point

and a new profile obtained.

(8) From this new point the procedure of steps (5), (6), and (7) are repeated to obtain the next point.

(9) Eventually after many more repetitions of the above, the program has stepped around the streamline back to the starting position and then an entirely new equipotential is followed from another starting location on the dawn- dusk meridian.

(10) After eighteen (this number is arbitrary but has been sufficient for the job at hand) equipotentials have been followed, the data are plotted and contours drawn by hand through the plotted values.

5.3 Some Aspects of Aeronomy Relevant to Programming the Problem

A. The Universal Time Dependence

The asymmetry of the geographic and geomagnetic poles implies that the polar ionosphere morphology is universal time dependent. This follows from the fact that the electric fields are related to the magnetosphere and so to magnetic coordinates, whereas the photoionization rate depends on geographic coordinates. As can readily be imagined, this complicates the problem considerably.

Some previous authors (eg., Duncan, 1962) have proposed a universal time dependence of the central polar cap on the basis on ionosonde data. Whether or not the trough regions are subject to a universal time control has never been mentioned to this author's knowledge.

To study this effect the various time dependent transformations have been "frozen" at two times that relate approximately to two situations where the magnetic pole is, 1) closest to the sun and 2) farthest from the sun. These will be two extremes of maximum and minimum solar illumination of the polar cap ionosphere. The result will be an average of about 2-3 hours span around these chosen times.

B. The Electron Density Profile Calculation

The main results of this thesis relate to the ionosphere morphology over the polar region, and the peak F-region density value is alone sufficient to illustrate the results. Nevertheless the vertical density profile has been computed. The main reason is to obtain the density at the 500 km altitude so that the results of Park and Banks (1975) could be utilized for estimating the polar wind ionization loss.

The electron density profile has a peak at around 300 km altitude in the F region. At and below this peak the density is determined by photo-chemical reactions only (Rishbeth and Garriott, 1969). Above the peak, diffusion becomes most important and is responsible for an exponential decrease of electron density with altitude. The usual criterion for determining the relative importance of vertical diffusion is to examine whether this vertical transport will move the plasma through one scale height during its lifetime (Rishbeth and Garriott, 1969). Equating the recombination time constant with the time to diffuse through a scale

height yields $\beta = D/H^2$, (Whitten and Poppoff, 1971), where β is the electron loss rate, D is the diffusion coefficient and H the scale height of the neutral gas.

The above expression is used to define the peak density height in this thesis, then the photo-chemical equations are solved at that height to obtain the peak ionization density. Rishbeth (1967) used this technique and found the values were within 10% of the other methods that solved the full continuity equation (e.g. Gliddon and Kendall, 1962).

Above the F-region peak density, diffusion is important in governing the shape of the vertical density profile. The continual vertical diffusion of O^+ ions upward and out of the ionosphere at high latitudes (called the polar wind, see Chapter III) should have an additional effect on the density profile (Banks and Kockarts, 1973).

According to the polar wind theory (Chapter III), over the entire polar region we would expect upward field-aligned fluxes of ionization because in the polar cap the magnetic field lines are open. Further equatorward where large east-west plasma velocities are present, the field lines are either open or closed for no more than a few hours at the most. It is known that the time constant for filling closed flux tubes in the magnetosphere is greater than 24 hours (Carpenter, 1973). Thus for the high latitudes of interest, there will be a continual upward flux, irrespective of whether the field lines are open or closed. Accepting this and turning to the polar wind theory (Banks and Kockarts, 1973), it is

noted that under the expected conditions of upward flux, the ionization density will fall off according to the neutral scale height. However, contrary observations of density profiles by the Chatanika incoherent scatter radar indicate a vertical change according to the plasma scale height which corresponds to diffusive equilibrium (Banks and Kockarts, 1973). In accordance with these observations, the ionization profile above the peak has been assumed in this work to be an exponential curve depending on the plasma scale height.

The use of the diffusive equilibrium ionization profile at altitudes higher than the F-region peak possibly results in a small overestimate of the polar wind ionization loss. The results of polar wind ionization loss were shown in Chapter III to be numerically small compared to chemical recombination. The main purpose of introducing this discussion of the ionization density profile at high altitudes is for evaluating the relative effect of the polar wind. Hence, as the polar wind is shown to be relatively unimportant, the high altitude profile is not relevant to any conclusions of this thesis, which relate to the peak ionization densities around 300 km altitude.

C. Errors in the Computed Electron Density Related to Temperature Changes and Vertical Drifts

Either a temperature variation of the thermosphere or a vertical component of an ionization drift can produce changes in the peak electron density and altitude of the peak electron density. Ionization drifts may be produced either directly by an electric field, or indirectly as a result of a neutral wind.

In this section we wish to estimate possible changes in the peak F-region electron density that result from thermal changes and vertical drifts. First we will mention thermal effects, second vertical drifts.

The effect of thermal variation has been evaluated by hand calculations. When the thermospheric temperature changes, a corresponding change in the neutral particle density profile subsequently affects both the electron loss rate and the diffusion coefficient. The magnitude and altitude of the peak ionization density were calculated for model atmospheres with 1000 and 1250 °K thermopause temperatures as indicated in the previous section of this chapter. This change of 250 degrees causes an altitude change of about 25 km and the peak density changes by a factor of about one and a half. Computations by Park and Banks (1974) for their 1000 °K thermosphere model give about a 50 km height increase when the temperature is increased by 250 degrees and a density increase of a factor three.

Although these variations are possible, such temperature changes occur (e.g. Watkins and Banks, 1974) only in association with large geomagnetic disturbances, a situation which does not apply to this thesis.

The second method for producing small peak density variations is by a vertical drift that can take place in conjunction with the inclined magnetic field. Although it is an irrelevant process close to the geomagnetic pole (where the magnetic field is nearly vertical), elsewhere a southward ion or neutral motion can result in a vertical ion velocity component. For example, if there is a horizontal southward ionization velocity of 400 m/s at a location with a 20 degree magnetic field dip angle, this would produce a change in the peak density by a factor of about one and one half. This estimation has been inferred from the work of Park and Banks (1974) for their 1000 degree thermosphere model.

There is also the possibility of a vertical component of the neutral motion. Rieger (1974) has analyzed 23 high latitude barium releases for vertical neutral drift velocities. He found 17 with zero velocity, and with one exception (42 m/s with large error bars of 20 m/s) the velocities were about 25 m/s. Only one data point showed a downward directed motion. Vertical ionization drifts induced by neutral motions of these magnitudes induce changes in electron density even less than those mentioned above.

CHAPTER VI

THEORETICAL RESULTS OF COMPUTER MODEL

6.1 Comparison with Experiment

Before discussing detailed results of the computer model we will first present some sample results and compare them with experimental data. This verification is necessary to ensure confidence in the model.

Recollecting that the problem is only solved in the polar region outside the plasmasphere, it is useful to consider this region as two parts: First, the circumpolar trough region that is observed on the night side of the earth (e.g., Nishida, 1967). Second, the polar cap, i.e., the area inside the optical auroral oval.

Figure 6.1 gives the results for equinox at 1730 and 0530 UT for a symmetrical convection electric field pattern. In this and subsequent figures some of the contours have small dashed sections. These indicate regions of uncertainty in drawing the contours because of nearby singularities (see Chapter IV). Note also that these figures are actually time averages around the times of maximum and minimum solar diurnal illumination. The next diagram (6.2) shows data from Nishida (1967), who averaged three months of low sunspot number equinoctical data obtained by the Alouette top side sounder satellite. Note in this figure the crescent-shaped contours of low electron densities on the night side of the earth near 60 degrees invariant latitude. This region is usually called the "main trough" or "midlatitude trough" e.g. Muldrew (1965), Sharp (1966). These

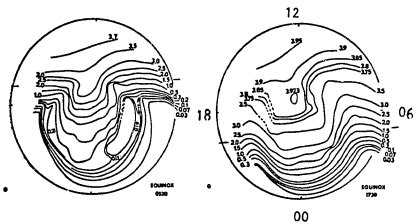

Figure 6.1 Plots of computed F-region electron density contours in invariant latitude-magnetic local time.
In this and all subsequent results the circle refers to 60^{o} invariant latitude, and magnetic time is denoted on the right hand diagram above.

The two small bars either side of the circle denote the line of zero solar depression angle.
The units of electron density are 10^{5} cm^{-3}.
The contours refer to the peak F region densities.

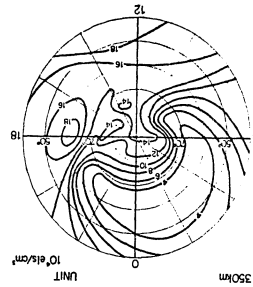

Figure 6.2 Experimental data from Nishida (1967). Note that this figure has been inverted to facilitate a comparison with the computed morphology. The data are from satellite top-side sounder records and represent near-peak densities in the altitude profile (350 km). These data include mid-latitudes (down to 40 degrees in this diagram), whereas the computed model illustrated stops at 60 degrees latitude.

data of Figure 6.2 apply to invariant latitudes from the north pole to 40 degrees, whereas the computer model (Figure 6.1) does not extend to latitudes below 60 degrees.

Comparing these figures (6.1 and 6.2) in terms of absolute magnitude of the electron density, the 70 degree latitude density at midnight according to Nishida's data (Figure 6.2) takes a value of 0.5×10^5 cm^{-3} at 350 km. The model (Figure 6.1) gives 0.3×10^5 cm^{-3} at 0530 UT and 1.5×10^5 at 1730 UT at 300 km. These values are thus a good match, considering the data averaging of Nishida.

Further equatorward (around 60° invariant latitude) the model predicts values a little more than 10^3 cm^{-3} which are a factor of two or three less than ground based ionosonde data show at trough minimum. This is related to uncertainties in determining the electron loss rate at densities less than 10^4 cm^{-3} when the loss rate is dependent on the electron density (see Chapter III). Such errors only apply for the lowest densities and do not affect any conclusions of this work. Further south, higher electron densities prevail due to replenishment from the plasmasphere. However, these lower latitudes are not a topic of this investigation and have not been included in the calculation here.

So far only the equinox data have been discussed; however, as will be seen later in data from the model (Figure 6.5), the troughs are more pronounced toward winter than summer. This is in agreement with Nishida (1967).

Turning now to the polar cap region, the computer model predicts a significant universal time dependence due to non-coincident geo-

graphic and geomagnetic poles and it is therefore unwise to associate these model values with Nishida's average because he averaged his data over all universal times. In fact, his value at the magnetic pole agrees well with the 0530 UT model plot but is not so good at 1730 UT (differs by a factor of about two). An optimum correspondence would require most of the satellite data to be taken around 1800 UT.

As a further comparison of this central polar cap region, data from Thule, Greenland, and Resolute Bay, Canada, (both close to the invariant magnetic pole) are presented in Figure 6.3. This diagram shows a broad peak around 1900 UT in the Thule data. The model data at the invariant pole for December 21, February 11, and March 21 fall within the given observed Thule ionosonde data values with the exception of February and winter at times of minimum diurnal photoionization. This period however was fairly disturbed; average sunspot number was high and Kp never stayed below 3 for extended periods of time. The Resolute data (Figure 6.3) were chosen from the most quiet periods of the available data and show good agreement.

Nishida (1967) comments in relation to the polar cap that "the density is a maximum in summer and a minimum in winter". This is in agreement with the result of Thomas (1963) that the winter anomaly (i.e., higher density in winter than in summer) does not occur when the sunspot number is less than 100. The computer model also shows bigger densities in summer than winter, and Nishida's results serve also to justify these model data.

The results of this thesis do not apply to high sunspot conditions where the midday electron density is larger in winter than summer.

	MID-SUMMER	EQUINOX	FEBRUARY 11	MID-WINTER	
DIURNAL MINIMUM DENSITIES (UNITS ARE 10^5 cm^3)	3.92	2.00	0.300	0.17	COMPUTER MODEL VALUE
	3.22---4.00	1.27	0.28---0.78	0.20---0.80	IONOSONDE VALUE
DIURNAL MAXIMUM DENSITIES (UNITS ARE 10^5 cm^3)	4.08	3.85	3.00	1.00	COMPUTER MODEL VALUE
	3.35---4.71	4.31	2.00---5.30	1.12---3.10	IONOSONDE VALUE
	(6/28/71)	(3/19/72)	(2/75)	(12/24-31/72)	

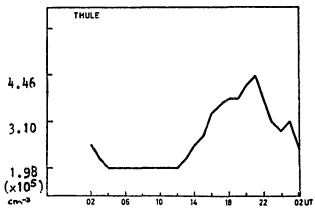

Figure 6.3 A comparison of computed model densities in the central polar cap with data from Resolute Bay, Canada, and Thule, Greenland.
Top: Model data comparison with ionosonde data from Resolute Bay. The quietest periods were chosen for comparison.
Bottom: Data average (November, 1969--March, 1970) for Thule ionosonde data. This is not a particularly quiet period but data illustrate the diurnal variation well (after Strömman and Maehlum, 1974).

These conditions could not be studied because the mechanisms responsible for this are unknown (Rishbeth, 1969).

6.2 The Universal Time Dependence of the Polar Cap and Trough Regions

Since the geographic and geomagnetic poles are separated by about ten degrees of latitude, it is proposed here that this fact should produce significant asymmetry in the polar cap and trough region ionosphere morphology. Motions of ionization over polar regions are controlled by large scale electric fields which originate in the magnetosphere. These electric fields are controlled by the interplanetary magnetic field direction and are thus ordered in geomagnetic latitude-magnetic time coordinates. The geographic pole rotates around the geomagnetic pole once per 24 hours so that a parcel of plasma traversing a certain path (defined by the $\vec{E} \times \vec{B}$ drift) over the polar region will be subjected to different photoionization rates depending on the universal time. The universal time gives the orientation of the rotating earth beneath the convective electric field pattern which can be considered fixed in space. It is a target of this work to examine this effect.

6.2.(a) The Polar Cap

As far as the polar cap is concerned, a universal time dependence is not a new suggestion. Duncan (1962) noted from his study of ionosonde data that "electron densities above Antarctica vary with universal time. Similar, but weaker, behavior is found above the Arctic." He speculated a possible explanation to be an increased flux of ionizing particles possibly due to some tidal effect. Hill (1963) and Hill and

Penndorf (1959) mention a maximum in electron density observed at Thule, Greenland, at 1700-2100 UT in agreement with the data of Strömman and Maehlum shown in the previous section of this chapter. King et al. (1968, 1971) discuss the time dependence of the Antarctic polar cap F region and offer an explanation in terms of neutral winds. Challinor (1969) also discusses this theory. They propose that vertical drifts of ionization occur due to the interaction of neutral winds with the inclined magnetic field. A vertical drift of ionization increases the lifetime of the ions (lower recombination rate with increasing altitude) so that a higher density can be maintained. As Strömman and Maehlum (1974) point out, this theory does not explain how ionization is generated, only how the ionization is maintained. These latter authors also rule out the low energy particle input mechanism on the basis of their optical observations. In summary, they conclude that no satisfactory explanation has been proposed for explaining the maintenence of the polar cap ionosphere in winter. They did not, however, recognize the paper of Sato and Rourke (1964) who noted that a similarity existed between contours of electron density and ionospheric currents, concluding that transport associated with these current systems could produce enhanced F-region densities at the poles in the absence of photoionization. This provided substance for Sato's earlier observation (Sato, 1959) that a tongue of ionization existed over the pole into the night side implying transport from the sunlit region. Knudsen (1974) then proposed that the diurnal cycle of solar zenith angle around the polar cleft latitudes near noon would be an explanation. He recognized that the solar zenith angle is a

minimum (maximum photoionization rate) around 1700 UT in the Arctic and suggested this plus transport could explain the UT effect.

This latter point of view corresponds with this author's, except that for most of the year the entire polar cap ionosphere undergoes significant UT-dependent variations in the photoionization rate and not just the cleft region. Further, it is not possible to say that this latter point of view is solely correct without numerical computations. For example, it may be that these diurnal variations are numerically too small compared with observations, and King's wind theory then acts to produce higher densities. To settle this dispute the computer model in this thesis has been used to compute ionization densities in the central northern polar cap without any vertical drifts: First, to check the overall morphology, and second, to compute the diurnal range of density values. Comparison of diagrams 6.1 and 6.2 indicates similar morphology. Data from Resolute Bay, Canada, and Thule, Greenland, (very close to the invariant pole) have been used as a checkpoint for the polar cap values and were discussed in the previous section (Figure 6.3).

There seems to be a good correspondence between the model values and the data from Thule and Resolute. It is noted that as winter approaches the model values are on the low side of observations, especially when the diurnal photoionization is a minimum. However, at these times the polar cap ionosphere is dominated by polar cusp particle input rather than transport of photoionization from the dayside of the earth. As was discussed in Chapter II there is some uncertainty in the polar cusp particle input used in the model and

possible increases in the polar cap densities could easily be obtained by varying the cusp particle input.

The main point to be made here is that simple transport of either photoionization or polar cusp auroral particles is sufficient to maintain the polar cap ionosphere. Without this transport the density would be much less, especially near winter when direct photoionization is very small or perhaps zero. Near midwinter there is negligible production of ionization in the polar cap region. However, electron densities are maintained at values around 1--2 x 10^5 cm^{-3} due to transport of ionization from the dayside of the earth. If this transport were absent the local ionization density in the polar cap can be estimated from assuming an equilibrium situation (production equals loss) when there is a very small photoionization rate. For example, under the condition of 10 degrees solar depression angle the photoionization rate is approximately unity at 300 km altitude. This results in an electron density of about 10^4 cm^{-3}, which is at least an order of magnitude less than computer model values and observations. The condition of negligible photoionization rate near midwinter would probably result in ionization densities considerably less than 10^4 cm^{-3}. It does not seem necessary to invoke any other mechanism to account for 1) a diurnal change and 2) the magnitudes of this diurnal change of ionization density. In summer, both the model and observations show very little diurnal change. This is because photoionization is dominant over the entire polar region at this time of year.

It can be concluded that horizontal anti-solar transport of ionization alone can provide the necessary polar cap ionization and account for its diurnal variation. While the work of King et al., (1968, 1971) and Challinor (1969) may certainly be applicable, it seems that the numerical effect of their mechanism is of secondary importance.

6.2(b) The Trough Region

The model indicates differing trough morphologies at different universal times of the day. Figure 6.1 shows a longitudinally much longer trough around the UT of minimum solar illumination over the polar cap. For this condition of lower photoionization, there is evidence for a shallow depression just poleward of an auroral peak, on the dawn side of the diagram. Whether one calls this a trough is a matter of definition, certainly it is insignificant compared with the main trough region.

Muldrew (1968) in his electron density contour plots shows a "high latitude trough" located similarly a few degrees north of the main trough on the dawn side of the earth only. Muldrew's data are noted only for the purpose of pointing out that such computed depressions are not inconsistent with observational data. In both the model and data, this short depression or high latitude trough is bounded by an auroral peak to the south and higher densities in the central polar cap.

6.3 Effects of Polar Cap and Trough Morphologies with Changing Global Convective Electric Fields

Figure 6.4 is a composite containing six plots of electron density contours corresponding to variations in both the global convective

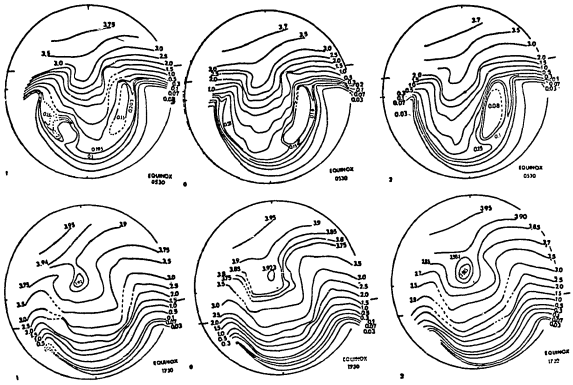

Figure 6.4 Plots of electron density contours showing changes resulting from varying the polar cap electric field morphology and the diurnal effect. Upper row is for minimum diurnal photoionization rate. Lower row is for maximum diurnal photoionization rate. Left to right indicates varying electric fields (see text).

electric field pattern (discussed in Chapter IV) and changes in the universal time for equinox. The top row of three plots represents data for approximate minimum daily solar illumination. The bottom row for approximate maximum solar illumination and near maximum of the polar cap diurnal density variation. The two diagrams on the left (with code '1') are for the asymmetric electric field condition where ionization speeds are faster on the dawn than dusk side of the polar cap. The center two diagrams (with code number '0') represent the symmetrical case. The two diagrams on the right are for electric field asymmetry, producing faster flow on the dusk than dawn side (see Chapter IV).

6.3(a) The Polar Cap Effects

Across the polar cap, tongues of ionization are present that extend from the day to night side of the earth over the pole. This feature is present in all model data shown in Figure 6.4. On the night side of the earth these tongues are skewed right or left depending on the symmetry of the polar cap electric field. For example, in the upper left plot of Figure 6.4 the antisolar directed speed of ionization is faster on the dawn side of the polar cap; thus ionization is carried further over into the night side of the earth on the dawn side of the polar cap. This skewing effect of the electron density contours in the polar cap is more marked at the universal time when the solar illumination is minimum.

The values at and close to the invariant pole are consistent with the changing electric field configuration at constant universal time. However, it may be expected, on the basis of Figure 6.4, that ground stations at some locations on the night side of the polar cap may experience changes by a factor of two in response to the three different global electric field patterns. This is especially apparent in locations just poleward of the main trough in the 0530 figures.

The small depression in electron density on the dawn side of the polar cap (upper right of Figure 6.4) deepens in response to slower ionization speeds on that side of the polar cap. The depression (upper left plot on Figure 6.4) tends to fill when speeds are larger on the dawn side of the polar cap.

A low peak is evident only at the time of day when photoionization is a minimum (top row of Figure 6.4). This is a result of the relative magnitudes of auroral and photoionization terms in the continuity equation. As the type of convection pattern is changed from the symmetrical case (center top of Figure 6.4) to asymmetrical case with lower velocities on the dawn side of the polar cap (top right of Figure 6.4) the auroral peak becomes more prominent on the dawn side of the polar cap. This is because all photoionization orginating from the polar cap region has had adequate time to decay, resulting in auroral particle precipitation dominating the production of ionization. Similarly, an auroral peak is evident on the dusk side of the polar cap when speeds of ionization are slower (top left of Figure 6.4) there. These night side auroral peaks are evident only

when the magnitude of the electron density is low (about 0.15×10^5 cm^{-3}).

A more persistent auroral peak could possibly be produced from higher auroral particle inputs. The data in Figure 6.2 from Nishida (1967) show no nightside auroral peak, because he notes that although auroral peaks were observed in his data "these were smoothed out in the averaged data since they are small both in occurrence frequency and in magnitude".

6.3 (b) The Trough Effects with Changing Polar Cap Electric Field Symmetry

Referring once again to Figure 6.4, the region which has become known as the main trough is seen on the night side of the earth as a crescent shape of low densities. There are no significant changes in the trough, either in overall morphology or in ionization density, corresponding to changing symmetry in the convective electric field pattern. Although not readily discernible from the figures there are small differences (up to 0.5×10^4) in the region immediately equatorward of the auroral oval; however, the overall global trough morphology shows no gross changes in response to these electric field changes.

6.4 Seasonal Effects

In this section we will show the effects of season as time moves away from the equinox. The variable involved is the solar photoionization. The line of zero solar depression angle moves about ten degrees toward and away from the sun each 24 hours, its diurnal average location being near the invariant pole at the equinox. As the season progresses toward winter, this average location moves away from the sun and vice versa for summer.

Figure 6.5 compares the equinox model data with data for February 11. It can be seen that the tongue of ionization from the dayside ionosphere is not so prominent in February as compared with that at the equinox. The polar cap densities are smaller on February 11 as compared to the equinox due to the lowered photoionization rate. The trough latitude near midnight is approximately the same for both months. However, the longitudinal extent of the trough on February 11 is nearly doubled by comparison with the equinox (for the condition of constant universal time). The auroral peaks are more prominent when the photoionization decreases.

To illustrate the effect of the variation of solar illumination on the polar cap, four situations are displayed in Figure 6.6. One extreme is when the line of zero solar depression angle is on the night side of the earth (midsummer). The electron densities are evenly high over the entire polar region with only a small gradient from day to night. In this situation, motions of ionization have relatively little effect on the overall morphology. The contours at some places have been difficult to draw because of the very small gradients. For this time of small gradients and little temporal variation a low auroral

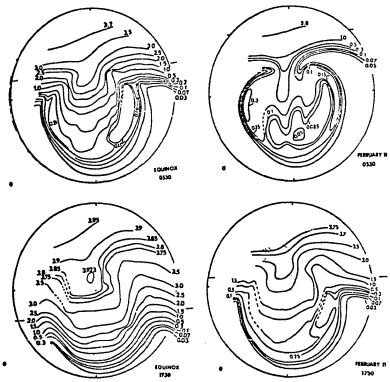

Figure 6.5 Model data for equinox and February 11. Upper two diagrams are for approximate minimum diurnal solar illumination. Lower two diagrams are for maximum diurnal solar illumination.

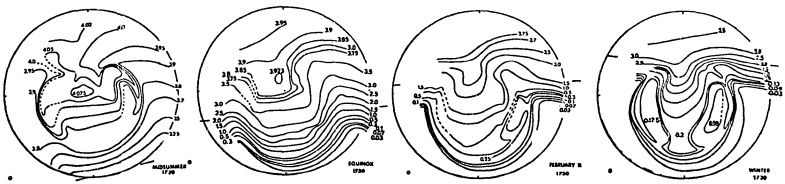

Figure 6.6 Four times of the year showing gradual seasonal transition of computed electron density contours. All other parameters are maintained constant.

peak is evident. As mentioned in a previous section, the data from Resolute show no significant diurnal variation at midsummer, and the observed density is close to that from the model at the invariant pole.

At the equinox the line of zero solar-depression angle has moved further toward the sun, so that on the night side of the earth ionization decays causing a trough. Photoionization is much greater than auroral ionization at the equinox time, so that no auroral effect is seen in the contours. There is a tongue of ionization that extends over the polar cap from the dayside.

Further toward winter (February 11) the tongue of ionization has withdrawn toward the dayside as a result of the lowered polar cap photoionization rate. The ionization in the trough moves further east-west toward the dayside of the earth before being built up by photo-ionization, resulting in a longer trough structure. A low auroral peak is evident on the dawn side of the earth with a depression poleward of this peak.

Comparing the February with the winter plot, the situation is similar but more extreme. Polar cap densities are less, the trough lengthens east-west, and the auroral peak on the dawn side of the earth is more prominent. An auroral peak is clear on this winter plot. The reason for an auroral peak occurring on the dawn side before the dusk side of the earth as season progresses toward winter is probably related to the nature of the polar plasma motions. Referring to Figure 4.6 the effect of the corotation of the earth is such that motions on the evening sector of the earth have a much larger equatorward component than the morning sector. The resultant effect is that a parcel of moving plasma tends to spend more time under the influence of

auroral particle precipitation on the morning side of the earth. The depression of densities poleward of the auroral precipitation tends to visually emphasize the presence of the auroral effect in these diagrams; however, the auroral peak is not large in terms of relative number densities, except in midwinter.

For all times of the year except midsummer, the trough model calculations show little variation in latitude and depth; with the only major changes in longitudinal extent. At summer the trough tends to fill but is still evident. Although Nishida's study of satellite data concentrated on equinox, some seasonal changes of the trough near midnight were shown. He also found from his data that the trough latitude did not change significantly during the year. The winter and equinox trough were very similar in depth but a little wider in winter; his summer data show a much shallower trough.

CHAPTER VII

SUMMARY

In this chapter an overall summary is presented to draw together all conclusions and significant statements from this work.

The main objective has been to construct a computer model of the polar F-region ionosphere. All the relevant production and loss functions have been examined and included. Horizontal transport resulting from the large scale convective electric fields is also taken into account. If such a model reasonably simulates the observed electron density morphology, then conclusions can be drawn about the importance of convection and the other mechanisms. The model can then be used to investigate consequent changes from varying individual parameters. The effects of 1) a varying polar cap electric field, 2) the separation of geographic and geomagnetic poles, 3) season, are studied with the model.

7.1 Results and Conclusions of the Computer Model

For the polar cap region it has been found that the horizontal transport of ionization from the dayside of the earth is responsible for the maintenance of the nighttime ionosphere, especially near mid-winter when the photoionization rate is very small. At these times of the year, if no plasma convection were present, the ionization densities could possibly fall to values an order of magnitude or more below 10^4 cm^{-3}, whereas in fact densities are not generally observed to fall below about 2×10^4 cm^{-3} even at mid-winter. This horizontal transport is also important at most other times of the year except near mid-summer when photoionization is the dominant factor over the entire polar region.

The electron density trough that has been observed to form on the nightside of the earth, just equatorward of the auroral oval, is also

simulated by the computer model. The trough is formed by chemical recombination in conjunction with the convective electric fields. This work has shown that the presence and morphology of these electric fields is critical in the formation of the ionization trough because the electric fields determine the paths followed by the ionization as it recombines.

Following the success of the model to simulate the polar cap and ionization trough, some of the model parameters were varied to investigate their effects. These, plus other detailed results of the model, are discussed below.

A. Polar Cap Electric Field Effects

Varying the asymmetry of the polar cap electric field has negligible effect on the ionization trough morphology and number density. However, inside the polar cap the morphology is changed and at some locations the ionization density varies by a factor of about two.

Depending on the time of day, and day of year, there may be a depression in the electron density (this may correspond to the high latitude trough described in the literature; Muldrew, 1965), located inside the polar cap just equatorward of the auroral precipitation region. The depth of these depressions depends on the asymmetry of the large scale polar cap electric field.

B. Effects of Geographic Pole-Geomagnetic Pole Separation

The separation of the geographic and geomagnetic poles is responsible for the universal time dependence of the polar cap ionization density. The density is approximately a maximum when the geomagnetic pole is nearest to the sun (the condition of maxi-

mum photoionization rate).

The ionization trough that lies equatorward of the auroral oval on the nightside of the earth also experiences diurnal changes due to the geomagnetic pole - geographic pole separation. The main result is a variation of the longitudinal extent of the trough. For example, during the months of February and March the longitudinal length of the trough has a diurnal variation of a factor of nearly two.

C. Seasonal Effects

As season progresses toward mid-summer the polar cap ionization densities increase to higher values. The densities increase by a factor of four from winter to summer. In addition, at mid-summer there is no significant diurnal density variation because of the constant photoionization rate over the entire polar region. The lowered photoionization rate near mid-winter results in the nighttime auroral precipitation becoming a dominant factor in the continuity equation, and hence, auroral precipitation is noted in the electron density contours.

The latitude and depth of the electron density trough changes very little with season, except near mid-summer when the trough tends to "fill". The major seasonal difference in the trough is an increase in its longitudinal extent, with a lengthening toward winter.

7.2 Other Conclusions Related to the Aeronomy of the Problem

A. The Velocity Dependent Electron Loss Rate

The velocity dependence of the reaction $O^+ + N_2 \rightarrow NO^+ + N$ can be ignored for conditions of low ion-neutral relative velocity such

as apply in this thesis. For conditions of high relative velocity, the electron loss rate is significantly increased by this reaction. These latter conditions may be present for example during geomagnetic storms.

B. Vibrationally Excited Nitrogen and the Electron Loss Rate

An equilibrium calculation of the quantity of vibrationally excited nitrogen in the aurora indicates that the associated change in the electron loss rate is insignificant.

7.3 Interpretations of Model Results

The most significant consequence of these results is that the electron density trough, even under the quietest possible steady state geophysical conditions, is not a static phenomena. The diurnal variation is most significant and has not been noted in the literature; further, many experimenters have not recognized the possible implications for their data. The earth is moving beneath a changing trough morphology so that two ground stations probing the ionosphere at the same magnetic latitude but different longitudes may "see" a different trough structure. Experiments that attempt to draw ionospheric electron density contours through the use of a meridian chain of ionosondes (e.g. Wagner et al., 1973) may produce misleading results because the results depend on the longitude of the meridian chain. Satellite ionospheric data are often ordered in terms of a magnetic disturbance index but with different universal times. Ordering data into sets of constant universal time could eliminate any possible distortion of the results. A similar criticism may be directed toward experiments involved in the polar cap; even though a universal time effect is well known to exist there, it has generally been ignored.

7.4 Outstanding Problems and Future Directions of Research

The basic limitation of this technique for modeling the polar ionosphere is the inadequate understanding of the polar electric fields. Although the average large scale pattern is well known for quiet times, the behavior of the electric fields, both time dependent, and for more disturbed periods, is most incomplete. It would, for example, be possible for this modeling method to give the time-dependent behavior of the ionosphere during auroral substorms. However, this would require detailed knowledge of both auroral particle precipitation and electric field morphology, both of which are now not available.

Extending this work to disturbed conditions where large ion-neutral relative velocities are present would demand a full knowledge of the neutral motions on a time dependent basis. This information is also lacking at this time.

REFERENCES

Akasofu, S. I., Polar and Magnetospheric Substorms, D. Reidel, Dordrecht - Holland, 1968.

Banks, P. M., Behavior of Thermal Plasma in the Magnetosphere and Topside Ionosphere, in Critical Problems of Magnetospheric Physics Proc. of COSPAR Symposium, 1972.

Banks, P. M. and G. Kockarts, Aeronomy, Acedemic Press, New York, 1973.

Banks, P. M., R. W. Schunk, and W. J. Raitt, NO^+ and O^+ in the High Latitude F Region, Geophys. Res. Letters, 1 , 239, 1974a.

Banks, P. M. and C. R. Chappell, A New Model for the Interaction of Auroral Electrons with the Atmosphere: Spectral Degradation, Backscatter, Optical Emission, and Ionization, J. Geophys. Res., 79, 1459, 1974b.

Bates, H. F., and R. D. Hunsucker, Quiet and Disturbed Electron Density Profiles in the Auroral Zone Ionosphere, Radio Science, 9, 455, 1974.

Bates, H. F. and T. D. Roberts, The Southward Midnight Surge in F-layer Wind Observed With the Chatanika Incoherent Scatter Radar, Accepted for publication J. Atmos. Terr. Phys., 1976(a).

Bates, H. F. and T. D. Roberts, A Technique for Using Incoherent Scatter to Estimate F-Region Zonal Winds During Joule Heating, Submitted to Planet. Space Sci., 1976(b).

Biondi, M. A., Charged Particle Recombination Processes, DNA Reaction Rate Handbook, Chapter 16, General Electric, California, 1974.

Bortner, M. H., R. H. Kummler, and T. Baurer, Summary of Suggested Rate Constants, DNA Reaction Rate Handbook, Chapter 24, General Electric, California, 1973.

Carpenter, D. L., and C. G. Park, On What Ionospheric Workers Should Know About the Plasmapause - Plasmasphere, Reviews of Geophysics and Space Physics, 11, 133, 1973.

Challinor, R. A., Universal Time Control of the Polar Ionosphere, Nature, Lond., 221, 941.

Chapman, S., The Absorption and Dissociative or Ionizing Effect of Monochromatic Radiation in an Atmosphere on a Rotating Earth, Proc. Phys. Soc. (London), 43, 26, 1931.

REFERENCES (Cont'd)

Caverly, R. S., A Correlation of Discrete and Diffuse Aurora with Particle Precipitation, PhD. Dissertation, University of Alaska, 1975.

Cook, G. R., M. E. Whitson, and R. J. Mc Neal, Temperature Dependence of the Quenching of Vibrationally Excited N_2 by O, EOS Transactions, AGU, 54, 403, 1973.

Duncan, R. A., Universal-Time Control of the Arctic and Antarctic F Region, J. Geophys. Res., 67, 1823, 1962.

Fedder, J. A. and P. M. Banks, Convection Electric Fields and Polar Thermospheric Winds, J. Geophys. Res., 77, 2328, 1972.

Fitzmaurice, J. A., Simplification of the Chapman Function for Atmospheric Attenuation, Appl, Optics, 3, 640, 1964.

Gliddon, J. E. C., and P. C. Kendall, A mathematical Model of the F2 Region, J. Atmos. Terr. Phys., 24, 1073, 1962.

Green, A. E. S., S. C. Lindenmeyer, and M. Griggs, Molecular Absorption in Planetary Atmospheres, J. Geophys. Res., 69, 493, 1964.

Gurnett, D. A., Electric Field and Plasma Observations in the Magnetosphere, in Critical Prcblems of Magnetospheric Physics, Proc. of COSPAR Symposium, 1972.

Heikkila, W. J. and J. D. Winningham, Penetration of Magnetosheath Plasma to Low Altitudes through the Dayside Mangetospheric Cusps, J. Geophys. Res., 76, 883, 1971.

Heppner, J. P., Electric Field Variations during Substorms, Planet. Space Sci., 20. 1475, 1972.

Heppner, J. P., High Latitude Electric Fields and the Modulations Related to Interplanetary Magnetic Field Parameters, Radio Science, 8, 933, 1973.

Hill, G. E., Sudden Enhancements of F-layer Ionization in Polar Regions, J. Atmospheric Sci., 20, 492, 1963.

Hill, G. E., and R. Penndorf, Research Concerning Forcasting Anomalous Propagation at High Latitudes, Sci. Rep. 3, Single Station and Synoptic Analysis of Ionospheric Data for the Arctic, Avco RAD-TR-59-19, AF19(604) - 4092, 1959.

Hinteregger, H. E., L. A. Hall and G. Schmidtke, Solar XUV Radiation and Neutral Particle Distribution in July 1963 Thermosphere, Space Research V, 1175, 1965.

REFERENCES (Cont'd)

Hunsucker, R. D., Chatanika Radar Investigation of High Latitude E-Region Ionization Structure and Dynamics, Radio Science, 10, 277, 1975.

King, J. W., H. Kohl, D. M. Preece, and C. Seabrook, An Explanation of Phenomena Occurring in the High Latitude Ionosphere at Certain Universal Times, J. Atmos. Terr. Phys., 30, 11, 1968.

King, J. W., D. Eccles, and H. Kohl, The Behaviour of the Antarctic Ionosphere, J. Atmos. Terr. Phys., 33, 1067, 1971.

Knudsen, W. C., Magnetospheric Convection and the High Latitude F2 Ionosphere, J. Geophys. Res., 79, 1046, 1974.

Lui, A. T. Y., D. C. Anger, D. Venkatesan, W. Sawchuk, and S. -I. Akasofu, The Topology of the Auroral Oval as Seen by the Isis-2 Scanning Auroral Photometer, J. Geophys. Res., 80, 1795, 1975.

Mc Farland, M. D. L. Albritton, F. C. Fehsenfeld, E. E. Ferguson, and A. L. Schmeltekopf, Flow-drift Technique for Ion Mobility and Ion-molecule Reaction Rate Constant Measurements II: Positive Ion Reactions of N^+, O^+, and N_2^+ with O_2 and O^+ with N_2 from thermal to 2ev, J. Chem. Phys., 59, 6620, 1973.

Muldrew, D. B., F-layer Ionization Trough Deduced from Alouette Data, J. Geophys. Res., 70, 2635, 1965.

Nagy, A. F. R. J. Cicerone, P. B. Hays, K. D. McWatters, J. W. Meriwether, A. E. Belon, C. L. Rino, Simultaneous Measurement of Ion and Neutral Motions by Radar and Optical Techniques, Radio Science, 9, 315, 1974.

Nishida, A., Average Structure and Storm-Time change of the Polar Topside Ionosphere at Sunspot Minimum, J. Geophys. Res., 72, 6051, 1967.

O'Neil, R. J., M. E. Whitson, Jr., and G. R. Cook, Temperature Dependence of the Quenching of Vibrationally Excited Nitrogen by Atomic Oxygen, J. Geophys. Res., 79, 1527, 1974.

Park, C. G. and P. M. Banks, Influence of Thermal Plasma Flow on the Mid-Latitude Nighttime F2 Layer: Effects of Electric Fields and Neutral Winds Inside the Plasmasphere, J. Geophys. Res., 79, 4661, 1974.

Park, C. G., and P. M. Banks, Influence of Thermal Plasma Flow on the Daytime F2 layer, G. Geophys. Res., 80, 2819, 1975.

Reasoner, D. L. and C. R. Chappell, Twin Payload Observations of Incident and Backscattered Auroral Electrons, J. Geophys. Res., 78, 2176, 1973.

REFERENCES (Cont'd)

Rees, M. H., Note on the Penetration of Energetic Electrons into the Earth's Atmosphere, Planet. Space Sci., 12, 722, 1964.

Rees, M. H., Private Communication, 1975.

Rieger, E., Neutral Air Motions Deduced from Barium Releases Experiments - I. Vertical Winds, J. Atmos. Terr. Phys., 36, 1377, 1974.

Rishbeth, H., The Effect of Winds on the Ionospheric F2 Peak, J. Atmos. and Terr. Phys., 2, 225, 1967.

Rishbeth, H., and O. K. Garriott, Introduction of Ionospheric Physics, Acedemic Press, New York, 1969.

Robertson, J. M., Hydrodynamics in Theory and Application, Prentice-Hall, 1965.

Sato, T., Morphology of Ionospheric F2 Disturbances in the Polar Regions, Rep. Ionos. Space Res. in Japan, 13, 91, 1959.

Sato, T. and G. F. Rourke, F Region Enhancements in the Antarctic, J. Geophys. Res., 69, 4591, 1964.

Schmeltekopf, A. L., F. C. Fehsenfeld, G. I. Gilman, and E. E. Ferguson, Reaction of Atomic Oxygen Ions with Vibrationally Excited Nitrogen Molecules, Planet. Space, Sci., 15, 401, 1967.

Schmeltekopf, A. L., E. E. Ferguson, and F. C. Fehsenfeld, Afterglow Studies of the Reactions He^+, $He(2^3S)$ and O^+ with Vibrationally Excited N_2, J. Chem. Phys., 48, 2966, 1968.

Schunk, R. W., and P. M. Banks, Auroral N_2 Vibrational Excitation and the Electron Density Trough, Geophys. Res. Letters, 2, 239, 1975.

Schunk, R. W., W. J. Raitt, and P. M. Banks, Effect of Electric Fields on the Daytime High-Latitude E and F Regions, J. Geophys. Res., 80, 3121, 1975.

Sharp, G. W., Midlatitude Trough in the Night Ionosphere, J. Geophys. Res., 71, 1345, 1966.

Stanley, G. M., Ground-based Studies of the F Region in the Vicinity of the Midlatitude Trough, J. Geophys. Res., 71, 5067, 1966.

Stromman, J. R., and B. N. Maehlum, Reconsideration of the Diurnal Variations in the Polar F Region Ionization, J. Atmos. Terr. Physics, 36, 1403, 1974.

REFERENCES (Cont'd)

Swider, W., and M. E. Gardener, On the Accuracy of Chapman Function Approximations, Appl. Optics, 8, 725, 1969.

Swift, D. W., and D. A. Gurnett, Direct Comparison Between Satellite Electric Field Measurements and the Visual Aurora, J. Geophys. Res., 78, 7306, 1973.

Thomas, J. O., The Electron Density Distribution in the F2 Region of the Ionosphere in Winter, J. Geophys. Res., 68, 2707, 1963.

Tulunay, Y. and J. Sayers, Characterictics of the Mid-latitude Trough as Determined by the Electron Density Experiment on Ariel III, J. Atmos, Terr. Phys., 33, 1737, 1971.

Wagner, R. A., A. L. Snyder, and S. -I. Akasofu, The Structure of the Polar Ionosphere During Exceptionally Quiet Periods, Planet. Space Sci., 21, 1911, 1973.

Watkins, B. J., and P. M. Banks, A Preliminary Study of High-Latitude Thermospheric Temperatures form Incoherent Scatter Radar Observations, J. Geophys. Res., 79, 5307, 1974.

Whitten. R. C. and I. G. Poppoff, Fundamentals of Aeronomy, Wiley, New York, 1971..

Wilkes, M. V., A Table of Chapman's Grazing Incidence Integral, Proc. Phys. Soc. (London), B67, 304, 1964.

APPENDIX

The following pages list the main program and associated subroutines used in this thesis. The next page presents a flow chart of the various functions performed.

If the operation within each block of this flow chart is carried out by a subroutine, the name of the routine is given in parentheses.

A brief description of each routine is contained in the Fortran listings.

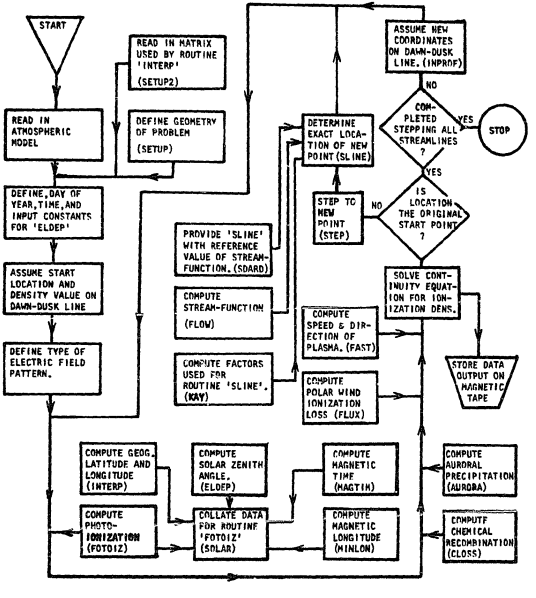

```
C
C     THIS IS THE MAIN PROGRAM--------------------
C THE FUNCTION IS TO  MATHEMATICALLY DEFINE  A PLASMA CONVECTION PATTERN
C  IN THE INVARIANT LATITUDE MAGNETIC TIME FRAME...
C NEXT THE MAIN PROGRAM  FOLLOWS EACH STREAMLINE WHILE SOLVING THE EQUATION OF
C  CONTINUITY.
C     EACH OF THE SUBROUTINES  PERFORMS A FUNCTION AS SPECIFIED
C     IN EACH OF THE ROUTINES----------
C ..............IN THE FIRST SECTION THE ATMOSPHERIC MODEL IS READ IN .
C ....... NEXT THE MATRIX IS READ IN FOR TRANSFORMING FROM INVARIANT
C        TO GEOGRAPHIC  COORDINATES.. .
C    THE REMAINDER OF THE MAIN PROGRAM HAS  TWO  LOOPS.. EACH RUN THROUGH THE BIG
C LOOP CORRESPONDS TO ONE STREAMLINE...
C    EACH RUN THROUGH  THE SMALLER LOOP  CORRES PONDS TO ONE SMALL STEP ON A
C     STREAMLINE.
C
      REAL N2,NE,INT
      REAL MODEL(36,3)
      DIMENSION A1MV(72,10),UT(3),GST(3),RAC4),DC(4)
      REAL KK
      COMPLEX P1,P2,P3,P4,P5,P6,P7,P8,P9,PO,PA,PB,PC,PD,PE,PF,PG,PH,
     +Z1,Z2,Z3,Z4,Z5,Z6,Z7,Z8,Z9,ZO,ZA,ZB,ZC,ZD,ZE,ZF,ZG,ZH,ZI,IG,VELOC,
     +PL,PJ,ZL,ZJ
      COMMON S,D,K1,K2,K3,K4,K5,K6,K7,K8,K9,KO,KA,KB,KC,KD,KE,KF,KG,KH,
     +W,OFFSET,STEPP,PI,
     +P1,P2,P3,P4,P5,P6,P7,P8,P9,PO,PA,PB,PC,PD,PE,PF,PG,PH,IG,
     +RK1,RK2,RK3,RK4,RK5,RK6,RK7,RK8,RK9,RKO,RKA,RK9,RKC,RKD,RKE,RKF,
     +RKG,RKH,
     +SCALE,DO,REAC,EFAC,
     +PS11,PS12,PS111N,PS121N,Q1,Q2,Q3,Q4,V,VX,RRR,
     +WMIDL,LFLAG,AFLAG,
     +RKL,RKJ,KL,KJ,PL,PJ
      INTEGER STEPNO,AIF,AIG
C
C
C
      ZMAX = 300.
      HP = 180.
      AU200 = 0.
      AU250 = 0.
      AU300 = 0.
      AU350 = 0.
      AU400 = 0.
      DELT = 0.0
C
C
      PI = 3.141592654
      Q1 = 2.5
      Q2 = 2.4
      Q3 = 3.1
      Q4 = 3.5
      STEPP = 0.1
      SCALE = 944.
      ANG = (60.*PI)/180.
      W = C.)
      W = -7.2722052
C *W* IS ANGULAR VELOCITY OF EARTH INCREASED BY FACTOR E+06.
C ALL VELOCITIES ARE WORKED IN INVARIANT LONGITUDE,MAGNETIC TIME
C RECTILINEAR COORDINATES,AND VELOCITIES INCREASED BY E+06 FOR MATHEMATICAL
```

```
C CONVENIENCE,JUST REMEMBER TO DIVIDE FINAL VELOCITY BY E+06.
C
      OFFSET = 0.5
C
      S = 3.3
      D = 1.50
      AHOUND = D*1.7
      HBOUND = S*1.7
      FBOUND = D*0.69
      GBOUND = S*1.2
      HBOUND = S*0.5
C
      CALL SETUP
C
C
      CALL SETUP2(A,B,IDAY,UTFIX,UTTT,AINV,WIND,
     +GST,RA,DC,EOS,PI,SCALF,
     +SD,CHI,SIGMA,MODEL,Z,ICHI)
C
      KK = -12
C
      CALL PLOTST
C
      A = -0.1
      A9 = ABS(A)
      IF(A.EQ.-1.1)A=A-0.001
      A = A 0.2
      A = A 0 - OFFSET
C
C SET 'LFLAG' EQUAL 0 FOR FLOW SYMMETRY,1 FOR FASTER ON  DAWN SIDE,
C                                       2 FOR FASTER ON DUSK SIDE.
      LFLAG = 1
      LFLAG = 2
      LFLAG = 0
C
      A = A - 9.0100
      CALL INPROF(OP200,OP250,OP300,OP350,OP400,A)
      A = A + 0.0001
      WRITE(3,92)OP200,OP250,OP300,OP350,OP400
      WRITE(3,93)UTFIX,IDAY
   93 FORMAT(1H ,'ABOVE IS INITIAL PROFILE',5X,'UTFIX=',F9.1,'IDAY=',I5)
C
      V = -1.0
      IF(A.GT.-0.5.AND.A.LT.+0.3)GO TO 642
      V = -2.0
      IF(A.LE.-0.5.AND.A.GT.-0.6)GO TO 642
      IF(A.GE.+0.5.AND.A.LT.+0.6)GO TO 642
      V = -3.0
      IF(A.LE.-0.6.AND.A.GT.-0.9)GO TO 642
      IF(A.GE.+0.6.AND.A.LT.+0.9)GO TO 642
      V = -4.0
      IF(A.LE.-0.9.AND.A.GT.-1.3)GO TO 642
      IF(A.GE.+0.9.AND.A.LT.+1.3)GO TO 642
      J = 1.3
  642 CONTINUE
C
      CALL FACTOR(3.3)
      CALL PLOT(A,B,3)
C     CALL SYMBOL(A,B,.1,8,0.,-2)
      WRITE(3,333)A,B
```

```
  831 FORMAT(1H1,20X,'BEGINNING A CONTOUR',10X,'A=',E16.5,2X,'B=',E16.5)
      CALL KAY(A,B,KK)
      CALL FLOW(A,B,PSI)
      CALL FAST(A,B,DIREC,SPEED)
C     WRITE(3,832)DIREC
      DIREC = -1.570796
C 832 FORMAT(1H ,'DIREC=',E16.5)
C     WRITE(3,820)PSI,DIREC,SPEED,A,B
      PSI2IN = PSI2
      PSI1IN = PSI1
      STAND = ABS(PSI)
      STEPNO = 0
      IFLAG =0
      JFLAG = 0
      KFLAG = 0
      IS = 1
C LOOP---LOOP---LOOP---LOOP---LOOP---LOOP---LOOP---LOOP---LOOP---LOOP---LOOP--
  801 CONTINUE
      CALL AURORA(A,B,AU200,AU250,AU300,AU350,AU400)
C
      IF(KFLAG.EQ.1)GO TO 836
      IF(AU.EQ.0.0.AND.B.GT.0.0.AND.A.LT.-1.0)CALL CORRT(A,B,KK,PSI,
     *STAND,KFLAG)
  838 CONTINUE
C
      CALL KAY(A,B,KK)
      CALL FAST(A,B,DIREC,SPEED)
      SPEE = SPEED * SCALE * 1.00 E-05
C     WRITE(3,1000)SPEE,A,B
C1000 FORMAT(1H ,25X,'SPEED=',E16.5,'   A=',E16.5,'   B=',E16.5)
C
C
      DELT = 0.1 * SCALE / SPEE
      INT = DELT
C
      IF(STEPP.NE.0.1)DELT=DELT/4.0
C
    2 CONTINUE
      CALL FLUX(OP200,OP250,OP300,OP350,OP400,AINC,WIND,DELT)
C
      Z = 200.0
      QO = 1.6 E+03
      N2 = 4.23 E+09
      O2 = 2.63 E+08
      CALL SOLAR(A,B,IDAY,UTFIX,UTTT,AINV,WIND,
     *GST,RA,DC,EOD,PI,SCALE,
     *QO,CHI,SIGMA,MODEL,Z,QCHI)
      NE = OP200
      CALL CLOSS(N2,O2,NE,INT,CL,BETA)
      OP200 = OP200 - BETA*OP200*DELT + QCHI*DELT +  AU200*DELT
C
      Z = 250.0
      QO = 5.3 E+02
      N2 = 1.02 E+09
      O2 = 5.24 E+07
      CALL SOLAR(A,B,IDAY,UTFIX,UTTT,AINV,WIND,
     *GST,RA,DC,EOD,PI,SCALE,
     *QO,CHI,SIGMA,MODEL,Z,QCHI)
      NE = OP250
      CALL CLOSS(N2,O2,NE,INT,CL,BETA)
```

```
      OP250 = OP250 - BETA*OP250*DELT + QCHI*DELT + AU250*DELT

      Z = 300.0
      Q0 = 2.0 E+02
      N2 = 2.83 E+08
      O2 = 1.22 E+07
      CALL SOLAR(A,B,IDAY,UTFIX,UTTT,AINV,WIND,
     *GST,RA,DC,EOD,PI,SCALE,
     *Q0,CHI,SIGMA,MODEL,Z,QCHI)
      NE = OP300
      CALL CLOSS(N2,O2,NE,INT,CL,BETA)
      OP300 = OP300 - BETA*OP300*DELT + QCHI*DELT + AU300*DELT

      Z = 350.
      Q0 = 70.
      N2 = 8.35 E+07
      O2 = 3.02 E+06
      CALL SOLAR(A,B,IDAY,UTFIX,UTTT,AINV,WIND,
     *GST,RA,DC,EOD,PI,SCALE,
     *Q0,CHI,SIGMA,MODEL,Z,QCHI)
      NE = OP350
      CALL CLOSS(N2,O2,NE,INT,CL,BETA)
      OP350 = OP350 - BETA*OP350*DELT + QCHI*DELT + AU350*DELT

      Z = 400.
      Q0 = 25.
      N2 = 2.54 E+07
      O2 = 7.76 E+05
      CALL SOLAR(A,B,IDAY,UTFIX,UTTT,AINV,WIND,
     *GST,RA,DC,EOD,PI,SCALE,
     *Q0,CHI,SIGMA,MODEL,Z,QCHI)
      NE = OP400
      CALL CLOSS(N2,O2,NE,INT,CL,BETA)
      OP400 = OP400 - BETA*OP400*DELT + QCHI*DELT + AU400*DELT
      IF(OP200.LT.0.0)OP200=0.0
      IF(OP250.LT.0.0)OP250=0.0
      IF(OP300.LT.0.0)OP300=0.0
      IF(OP350.LT.0.0)OP350=0.0
      IF(OP400.LT.0.0)OP400=0.0


      RNMAX = (ZMAX - 250.)*(OP300 - OP250)/50.
      RNMAX = RNMAX + OP250
      IF(ZMAX.GE.300.)GO TO 76
      OP300 = RNMAX * EXP(-(300. - ZMAX)/HP )
   76 CONTINUE
      IF(ZMAX.GE.350.)GO TO 77
      OP350 = RNMAX * EXP(-(350.0 - ZMAX)/HP )
   77 CONTINUE
      IF(ZMAX.GE.400.)GO TO 78
      OP400 = RNMAX * EXP(-(400.0 - ZMAX)/HP )
   78 CONTINUE
      OP450 = RNMAX * EXP(-(450. - ZMAX)/HP )
      OP500 = RNMAX * EXP(-(500. - ZMAX)/HP )


      WRITE(3,92)OP200,OP250,OP300,OP350,OP400,RNMAX
   92 FORMAT(1H ,'DENSITY PROFILE IS',5E16.5,'  NMAX=',E16.5)
      WRITE(3,94)OP450,OP500,QCHI,EOD,A,B
   94 FORMAT(1H ,'OP450=',E16.5,'OP500=',E16.5,' QCHI=',E16.5,' EOD=',
```

```
     *F8.2,' A=',F8.2,' B=',F8.2)
C
C
C
      AAB = ABS(A)
      BAB = ABS(B-OFFSET)
      STEPP = 0.1
C     IF(AAB.LT.FBOUND.AND.BAB.LT.GBOUND.AND.BAB.GT.HBOUND)STEPP=0.025
C     IF(AB.GT.1.11)STEPP=0.025
C     IF(AAB.GT.ABOUND.OR.BAB.GT.BBOUND)STEPP=0.2
      STEPP = 0.1
      IF(A.LT.-2.2)STEPP=0.025
C
      CALL STEP(A,B,AN,BN,DIREC,STEPP)
C     WRITE(3,837)A,B,AN,BN,DIREC,STEPP
C 837 FORMAT(1H ,'FROM STEP',3X,'A=',E16.5,2X,'B=',E16.5,2X,'B=',E16.5,
C    *2X,'AN=',E16.5,2X,'BN=',E16.5,2X,'DIREC=',E16.5,2X,'STEPP=',E16.5)
      CALL SLINE(AN,BN,STAND,AP,BP,DIREC,KK)
      IF(WMIDL.EQ.1.0)GO TO 805
C
      IF(AP.NE.A)GO TO 826
      IF(BP.GT.B)GO TO 827
      DIREC = -PI*0.5
      GO TO 828
  827 DIREC = PI*0.5
      GO TO 828
  826 DIREC = ATAN( (BP-B)/(AP-A) )
      IF(AP.GT.A)GO TO 835
      IF(BP.LT.B)GO TO 836
      DIREC = PI + DIREC
      GO TO 828
  836 CONTINUE
      DIREC =-PI + DIREC
  828 CONTINUE
C
      A = AP
      B = BP
C     WRITE(3,814)A,B
C 814 FORMAT(1H ,'M','STEP OUTPUT',2X,'A=',E16.5,2X,'B=',E16.5)
C     WRITE(3,820)PSI,DIREC,SPEED,A,B
C 820 FORMAT(1H ,1X,'FLOW OUTPUT',2X,'PSI=',E16.5,2X,'DIREC=',E16.5,
C    *2X,'SPEED=',E16.5,2X,'A=',E16.5,2X,'B=',E16.5)
      DIST = IS * STEPP
      IS = IS + 1
C     WRITE(3,821)STEPNO
C 821 FORMAT(1H ,'STEPNO=',I5)
      YA = ABS(A)
      IF(YA.GT.D)GO TO 800
      IF(B.LE.-OFFSET)GO TO 800
      IFLAG = 1
  800 CONTINUE
      YB =ABS(A)
C
C NEXT TWO STATEMENTS SET THE PLOT LIMITS
      IF(YA.GT.14.)STEPNO=9999
      IF(YB.GT.10.)STEPNO=9999
C
      IF(A.GT.15.)GO TO 823
      IF(B.GT.15.)GO TO 823
      IF(B.GT.-OFFSET)JFLAG=0
```

```
      IF(B.LE.-OFFSET)JFLAG =1
      IF(IFLAG.EQ.1.AND.JFLAG.EQ.1)GO TO 805
  829 CONTINUE
C HAVE NOW COMPLETED ONE ITERATION.
C
C     WRITE(3,822)
C 822 FORMAT(1H ,'COMPLETED A DATA POINT')
C
      GO TO 825
  823 CONTINUE
      WRITE(3,824)
  824 FORMAT(1H ,'PROGRAM ORDERED TO STOP BECAUSE A,B GONE TOO LARGE')
      STEPNO = 9999.
  825 CONTINUE
C
C
      IF(STEPNO.GE.3)GO TO 805
      STEPNO = STEPNO + 1
      RNMAXX = RNMAX*(1.0 E-05)
      CALL PLOT(A,B,3)
      CALL NUMBER(A,B,0.32,RNMAXX,0.,3)
C     CALL PLOT(A,B,2)
C     CALL SYMBOL(A,B,0.1,3,0.,-2)
      GO TO 801
C LOOP---LOOP---LOOP---LOOP---LOOP---LOOP---LOOP---LOOP---LOOP---LOOP--
  805 CONTINUE
C XXXXXXXXXXXXXXXXXXXXXXXXXXXXXXXXXXXXXXXXXXXXXXXXXXXXXXXXXXXXXXXXXXXXXXX
C
  830 CONTINUE
      CALL PLOT(0.,0.,-3)
      STOP
      END
```

```
      SUBROUTINE SLINE(AN,BN,STAND,AP,BP,DIREC,KK)
C
C     THE PURPOSE OF ROUTINES 'SLINE' AND 'SDARC' IS TO FACILITATE THE
C        OF THE PLASMA FLOW.  IT DOES THIS BY STEPPING ALONG A STREAMLINE
C        DEFINED BY A VALUE OF THE STREAM-FUNCTION 'STAND'.
C     AFTER STEPPING FROM(A,B) TO (AN,BN) THE ROUTINE SEARCHES FOR A NEARBY
C     POINT ON THE STREAMLINE.  IN NOT TAKING SUCH PRECAUTIONS TO ENSURE
C     THE PLASMA PATH IS LOCKED ON TO A STREAM-FUNCTION SMALL ERRORS WILL
C     ADD UP TO RESULT IN UNACCEPTABLE DEVIATIONS FROM THE PROPOSED
C        PLASMA PATH.
C     'DIREC' IS THE DIRECTION OF PLASMA FLOW.  'KK' IS DEFINED IN ROUTINE
C                                                    -----'KAY'.
C
      REAL KK
      COMPLEX P1,P2,P3,P4,P5,P6,P7,P8,P9,PO,PA,PB,PC,PD,PE,PF,PG,PH,
     *Z1,Z2,Z3,Z4,Z5,Z6,Z7,Z8,Z9,ZO,ZA,ZB,ZC,ZD,ZE,ZF,ZG,ZH,Z,ZG,VELOC,
     *PL,PJ,ZL,ZJ
      COMMON S,D,K1,K2,K3,K4,K5,K6,K7,K8,K9,KO,KA,KB,KC,KD,KE,KF,KG,KH,
     *W,OFFSET,STEPP,PI,
     *P1,P2,P3,P4,P5,P6,P7,P8,P9,PO,PA,PB,PC,PD,PE,PF,PG,PH,IG,
     *RK1,RK2,RK3,RK4,RK5,RK6,RK7,RK8,RK9,RKO,RKA,RKB,RKC,RKD,RKE,RKF,
     *RKG,RKH,
     *SCALE,DD,RFAC,EFAC,
     *PSI1,PSI2,PSIIN,PSI2IN,Q1,Q2,Q3,Q4,V,VX,RRR,
     *NMIDL,LFLAG,MFLAG,
     *RKL,RKJ,KL,KJ,PL,PJ
      WMIDL = 0.0
      LIM = 200
C     WRITE(3,927)
C 927 FORMAT(1H ,100('*'),2X,'ENTERING ROUTINE SLINE')
C     WRITE(3,901)STAND
C 901 FORMAT(1H ,30X,'STAND=',E16.5)
      E = 0.05
      DELL = 4.36 E-03
      DELL = DELL * 2.0
      N = 0
  787 CONTINUE
C     WRITE(3,908)
C 908 FORMAT(1H ,30X,'DEL INCREASING')
C**********************************************************************
  703 CONTINUE
      DEL = N * DELL
      AP = AN -(STEPP*DEL * SIN(DIREC*(DEL/2.0)) )
      BP = BN + (STEPP*DEL* COS(DIREC*(DEL/2.0)) )
      A = AP
      B = BP
C
      CALL KAY(A,B,KK)
      CALL FLOW(AN,BN,PSI)
      CALL SDARC(A,B,STAND)
C     WRITE(3,963)N,PSI,A,B
C 963 FORMAT(1H ,30X,'N=',I5,2X,'PSI=',E16.5,' A=',E16.5,' B=',E16.5)
      ERRA = ABS(ABS(PSI)-STAND)
      PSIA = ABS(PSI)
      IF(ERRA.LE.E)GO TO 701
      N = N+1
      IF(N.GT.LIM)GO TO 702
      DEL = N * DELL
      AP = AN -(STEPP*DEL * SIN(DIREC*(DEL/2.0)) )
```

```
      BP = BN + (STEPP*DEL* COS(DIREC+(DEL/2.0)) )
      A = AP
      B = BP
      CALL KAY(A,B,KK)
      CALL FLOW(A,B,PSI)
      CALL SDARD(A,B,STAND)
C     WRITE(3,963)M,PSI,A,B
      ERRB = ABS(ABS(PSI) - STAND)
      PSIB = ABS(PSI)
      ADD = ABS(PSIA - PSIB)
      IF(ERRA.LT.ERRB)GO TO 702
      IF(ERRB.LE.E)GO TO 701
      M = M+1
      IF(M.GT.LIM)GO TO 702
      IF(ADD.LT.0.01)M=M+3
      IF(ADD.LE.0.005)M=M+4
      GO TO 703
C*****************************************************************
  701 CONTINUE
C     WRITE(3,962)M
C     WRITE(3,909)
C 909 FORMAT(1H ,30X,'A HIT FOR DEL INCREASING')
      RETURN
  702 CONTINUE
C     WRITE(3,962)M
C     WRITE(3,910)
C 910 FORMAT(1H ,30X,'NO RESULTS FOR DEL INCREASING')
  750 CONTINUE
      DELL =-4.36 E-03
      DELL = DELL * 2.0
      M = 1
C
C*****************************************************************
  753 CONTINUE
      DEL = M * DELL
      AP = AN -(STEPP*DEL * SIN(DIREC+(DEL/2.0)) )
      BP = BN + (STEPP*DEL* COS(DIREC+(DEL/2.0)) )
      A = AP
      B = BP
      CALL KAY(A,B,KK)
      CALL FLOW(A,B,PSI)
      CALL SDARD(A,B,STAND)
C     WRITE(3,963)M,PSI,A,B
      ERRA = ABS(ABS(PSI)-STAND)
      PSIA = ABS(PSI)
      IF(ERRA.LE.E)GO TO 751
      M = M+1
      IF(M.GT.LIM)GO TO 752
      DEL = M * DELL
      AP = AN -(STEPP*DEL * SIN(DIREC+(DEL/2.0)) )
      BP = BN + (STEPP*DEL* COS(DIREC+(DEL/2.0)) )
      A = AP
      B = BP
      CALL KAY(A,B,KK)
      CALL FLOW(A,B,PSI)
      CALL SDARD(A,B,STAND)
C     WRITE(3,963)M,PSI,A,B
      ERRB = ABS(ABS(PSI) - STAND)
      PSIB = ABS(PSI)
      ADD = ABS(PSIA - PSIB)
```

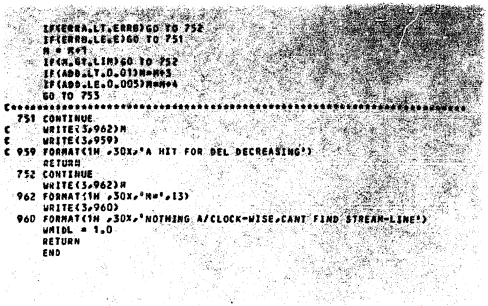

```
      IF(ERRA.LT.ERRB)GO TO 752
      IF(ERRB.LE.E)GO TO 751
      A = A+1
      IF(A.GT.LIM)GO TO 752
      IF(ADD.LT.0.013)H=H*5
      IF(ADD.LE.0.005)H=H*4
      GO TO 753
C*****************************************************************
  751 CONTINUE
C     WRITE(3,962)H
C     WRITE(3,959)
C 959 FORMAT(1H ,30X,'A HIT FOR DEL DECREASING')
      RETURN
  752 CONTINUE
      WRITE(3,962)H
  962 FORMAT(1H ,30X,'H=',I3)
      WRITE(3,960)
  960 FORMAT(1H ,30X,'NOTHING A/CLOCK-WISE,CANT FIND STREAM-LINE')
      WAIDL = 1.0
      RETURN
      END
```

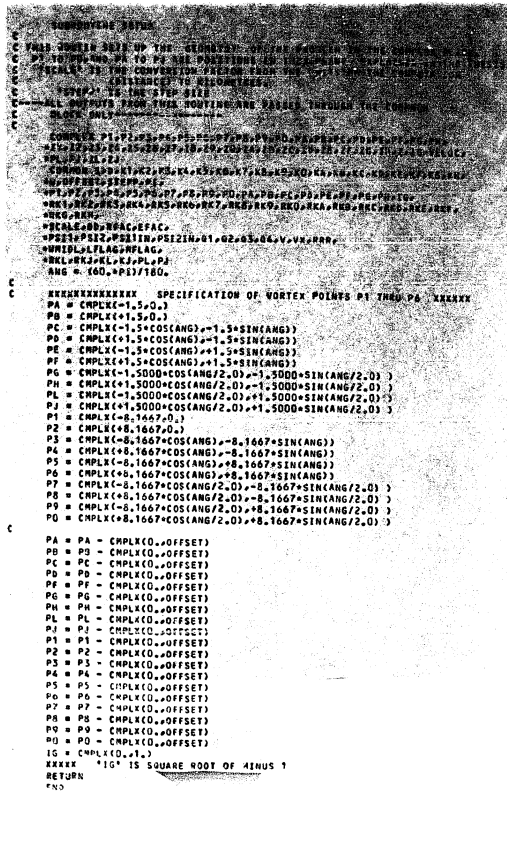

```
      SUBROUTINE VORTEX
C
C     THIS ROUTINE SETS UP THE  GEOMETRY  OF THE VORTICES ON THE CANARD AND
C     BY TURNING THE PX TO PZ THE PROJECTION ON THE X-Z PLANE.  FINALLY
C     'CALL' IS THE CONVERSION FACTOR FROM THE 'CYCLE' TO 'RADIAN'.
C     'DELTAT' IS THE TIME STEP SIZE.
C---ALL OUTPUTS FROM THIS ROUTINE ARE PASSED THROUGH THE COMMON
C     BLOCK ONLY-----------------------------
C
      COMMON P1,P2,P3,P4,P5,P6,P7,P8,P9,P0,PA,PB,PC,PD,PE,PF,PG,PH,PL,PJ,
     *IG,IP,IS,IT,
     *COMMON S,DELT,K2,K3,K4,K5,K6,K7,K8,K9,K0,K1,K6,K6,K6,K6,K6,K6,K6,K6,
     *K,DIFFERE,ZEEPP,PI,
     *P1,P2,P3,P4,P5,P6,P7,P8,P9,P0,PA,PB,PC,PD,PE,PF,PG,PH,PL,PJ,P1,P2,P3,
     *RK1,RK2,RK3,RK4,RK5,RK6,RK7,RK8,RK9,RK0,RKA,RKB,RKC,RKD,RKE,RKF,
     *RK0,RKM,
     *RCALC,RBC,RCAC,EFAC,
     *PSIE,PSIZ,PSIIN,PSIZIN,01,02,03,04,V,VM,RHO,
     *WMIN,LTLAG,RPLAG,
     *RKL,RMJ,RKL,KJ,PL,PJ
      ANG = 160.*PI)/180.
C
C     XXXXXXXXXXXXXX   SPECIFICATION OF VORTEX POINTS P1 THRU P0  XXXXXX
      PA = CMPLX(-1.5,0.)
      PB = CMPLX(+1.5,0.)
      PC = CMPLX(-1.5*COS(ANG),-1.5*SIN(ANG))
      PD = CMPLX(+1.5*COS(ANG),-1.5*SIN(ANG))
      PE = CMPLX(-1.5*COS(ANG),+1.5*SIN(ANG))
      PF = CMPLX(+1.5*COS(ANG),+1.5*SIN(ANG))
      PG = CMPLX(-1.5000*COS(ANG/2.0),-1.5000*SIN(ANG/2.0) )
      PH = CMPLX(+1.5000*COS(ANG/2.0),-1.5000*SIN(ANG/2.0) )
      PL = CMPLX(-1.5000*COS(ANG/2.0),+1.5000*SIN(ANG/2.0) )
      PJ = CMPLX(+1.5000*COS(ANG/2.0),+1.5000*SIN(ANG/2.0) )
      P1 = CMPLX(-8.1667,0.)
      P2 = CMPLX(+8.1667,0.)
      P3 = CMPLX(-8.1667*COS(ANG),-8.1667*SIN(ANG))
      P4 = CMPLX(+8.1667*COS(ANG),-8.1667*SIN(ANG))
      P5 = CMPLX(-8.1667*COS(ANG),+8.1667*SIN(ANG))
      P6 = CMPLX(+8.1667*COS(ANG),+8.1667*SIN(ANG))
      P7 = CMPLX(-8.1667*COS(ANG/2.0),-8.1667*SIN(ANG/2.0) )
      P8 = CMPLX(+8.1667*COS(ANG/2.0),-8.1667*SIN(ANG/2.0) )
      P9 = CMPLX(-8.1667*COS(ANG/2.0),+8.1667*SIN(ANG/2.0) )
      P0 = CMPLX(+8.1667*COS(ANG/2.0),+8.1667*SIN(ANG/2.0) )
C
      PA = PA - CMPLX(0.,OFFSET)
      PB = PB - CMPLX(0.,OFFSET)
      PC = PC - CMPLX(0.,OFFSET)
      PD = PD - CMPLX(0.,OFFSET)
      PE = PE - CMPLX(0.,OFFSET)
      PF = PF - CMPLX(0.,OFFSET)
      PG = PG - CMPLX(0.,OFFSET)
      PH = PH - CMPLX(0.,OFFSET)
      PL = PL - CMPLX(0.,OFFSET)
      PJ = PJ - CMPLX(0.,OFFSET)
      P1 = P1 - CMPLX(0.,OFFSET)
      P2 = P2 - CMPLX(0.,OFFSET)
      P3 = P3 - CMPLX(0.,OFFSET)
      P4 = P4 - CMPLX(0.,OFFSET)
      P5 = P5 - CMPLX(0.,OFFSET)
      P6 = P6 - CMPLX(0.,OFFSET)
      P7 = P7 - CMPLX(0.,OFFSET)
      P8 = P8 - CMPLX(0.,OFFSET)
      P9 = P9 - CMPLX(0.,OFFSET)
      P0 = P0 - CMPLX(0.,OFFSET)
      IG = CMPLX(0.,1.)
      XXXXX   'IG' IS SQUARE ROOT OF -1MINUS 1
      RETURN
      END
```

```
      SUBROUTINE BASIC(A,B,DIREC,VELOC)
C GIVEN ANY COORDINATE(A,B), THIS ROUTINE COMPUTES THE VELOC. (VELOCITY
C          DIREC(DIREC) OF THE PLANAR POTENTIAL FLOW AT THE POINT (A,B)
      REAL KK
      COMPLEX Z1,Z2,Z3,Z4,Z5,Z6,Z7,Z8,Z9,ZD,ZA,ZB,ZC,ZD,ZE,ZF,ZG,ZH,ZL,ZJ,
     *VELOC,Z,CMPLX
      COMMON
     *OFFSET,STAGE,I,
     *P1,P2,P3,P4,P5,P6,P7,P8,P9,PD,PA,PB,PC,PD,PE,PF,PG,PH,PL,PJ,
     *RK1,RK2,RK3,RK4,RK5,RK6,RK7,RK8,RK9,RKD,RKA,RKB,RKC,RKD,RKE,RKF,
     *RKG,RKH,
     *SCALE,XDD,YPAC,EPAC,
     *PSI1,PSI2,PSI3,PSI4,PSI2IN,01,02,03,04,VJVI,RRR,
     *WHOLE,XFLAG,MFI,AS,
     *RKL,RKJ,XL,XJ,PL,PJ
C     XXXXX  HERE CALCULATE SPEED AND DIRECTION OF FLOW XXXXXXXXXXXXXXX
C     XXXXX  DIREC IS ANGLE MEASURED -PI .LE. DIREC .LE. PI    XXXXXXXX
      Z = CMPLX(A,B)
      Z1 = RK1/(Z-P1)
      Z2 = RK2/(Z-P2)
      Z3 = RK3/(Z-P3)
      Z4 = RK4/(Z-P4)
      Z5 = RK5/(Z-P5)
      Z6 = RK6/(Z-P6)
      Z7 = RK7/(Z-P7)
      Z8 = RK8/(Z-P8)
      Z9 = RK9/(Z-P9)
      ZD = RKD/(Z-PD)
      ZA = RKA/(Z-PA)
      ZB = RKB/(Z-PB)
      ZC = RKC/(Z-PC)
      ZD = RKD/(Z-PD)
      ZE = RKE/(Z-PE)
      ZF = RKF/(Z-PF)
      ZG = RKG/(Z-PG)
      ZH = RKH/(Z-PH)
      ZL = RKL/(Z-PL)
      ZJ = RKJ/(Z-PJ)
      VELOC=(Z1+Z2+Z3+Z4+Z5+Z6+Z7+Z8+Z9+ZD+ZA+ZB+ZC+ZD+ZE+ZF+ZG+ZH
     *+ZL+ZJ)*1G
      VR = REAL(VELOC)
      VI =-AIMAG(VELOC)
C
C     XXX  NOW ADD CO-ROTATION VELOCITY  XXXXXXXXXXXXXXXXXXXXXXXXXXXXXX
      THETA = 1.570796327
      IF(A.EQ.0.)GO TO 38
      THETA = ATAN(B/A)
      IF(A.GT.0.)GO TO 30
   38 CONTINUE
      IF(B.LT.0.)GO TO 39
      THETA = PI - ABS(THETA)
      GO TO 30
   39 CONTINUE
      THETA = -PI + ABS(THETA)
   30 CONTINUE
C     ***************************************************************
      COLATT = RRR
      COLAT = (COLATT * SCALE )/111.
```

```
      SUBROUTINE STEP(A,B,AN,BN,DIREC,STEPP)
C
C   THIS ROUTINE STEPS FROM APOINT (A,B) TO A NEW POINT (AN,BN) IN THE DIRECTION
C    'DIREC' WITH A STEP SIZE 'STEPP'.
C
C     WRITE(3,1000)
C1000 FORMAT(1H ,100('T'),2X,'ENTERING ROUTINE STEP.')
C     XXX 'STEPP' IS THE STEP SIZE XXXXXXXXXXXXXXXXXXXXXXXXXXXXXXXXXXXXX
C
C     XXX   'A' AND 'B' ARE INVARIANT RECTILINEAR COORDINATES,
C           'AN' AND 'BN' ARE NEW COORDINATES COMPUTED
C           FROM A,B,AND DIRECTION OF PLASMA FLOW(DIREC),AFTER
C           TAKING STEP ALONG STREAMLINE 'PSI'.
C     XXXXXXXXXXXXXXXXXXXXXXXXXXXXXXXXXXXXXXXXXXXXXXXXXXXXXXXXXXXXXXXXX
      AN = A + (STEPP* COS(DIREC) )
      BN = B + (STEPP* SIN(DIREC) )
C     WRITE(3,1002)AN,BN
C1002 FORMAT(1H ,75X,'AN=',E16.5,2X,'BN=',E16.5)
C     WRITE(3,1001)
C1001 FORMAT(1H ,100('T'),2X,'LEAVING STEP')
      RETURN
      END
```

```
      SUBROUTINE ELDEP ( LAT, LONG, UT, GST, RA, DC, EOD )
C
C ROUTINE TO CALCULATE ELEVATION OR DEPRESSION ANGLE - USUALLY OF SUN
C OR MOON
C     INPUT     LAT     = LATITUDE OF OBSERVER DECIMAL DEGREES + NORTH
C               LONG    = LONGITUDE OF OBSERVER DEC. DEG. POSITIVE EAST
C               UT(3)   = UNIVERSAL TIME HR-MIN-SEC
C               GST(3)  = GREENWICH SIDERIAL TIME AT 0 HRS UT. HR-MIN-SEC
C               RA(4)   = RIGHT ASCENSION AT 0 HRS UT  HR-MIN-SEC-DSEC.
C                         DSEC = CHANGE IN SECONDS TO NEXT DAY
C               DC(4)   = DECLINATION AT 0 HRS UT  DEG-MIN-SEC-DSEC
C     OUTPUT    EOD     = ELEVATION OR DEPRESSION ANGLE OF BODY AT GIVEN
C                         UT TIME
C                         POSITIVE NUMBERS ARE ELEVATION ANGLES AND
C                         NEGATIVE NUMBERS ARE DEPRESSION ANGLES
C
      REAL                LAR
      REAL                LAT,            LONG,           LST
      DIMENSION           UT(3),          GST(3),         RA(4),
     1   DC(4)
C
      F(X1, X2, X3 ) = X1 + ( X2 + X3 / 60. ) / 60.
      DTR = 3.14159264 / 180.
C
C CONVERT EVERYTHING TO DECIMAL DEGREES
C
      GSD = F( GST(1), GST(2), GST(3) ) * 15.
      UTD = F( UT(1), UT(2), UT(3) ) * 15.
      FRD = UTD / 360.
      ALPD = F( RA(1), RA(2), RA(3) + RA(4) * FRD ) * 15
      DECD = F ( DC(1), DC(2), DC(3) + DC(4) * FRD )
C
C COMPUTE LOCAL SIDERIAL TIME
C
      LST = UTD * 1.002737 + GSD + LONG + 360.
      LST = AMOD ( LST, 360.)
C
C COMPUTE HOUR ANGLE
C
      HA = LST - ALPD
C
C COMPUTE ELEVATION OR DEPRESSION ANGLE
C
      HAR = HA * DTR
      LAR = LAT * DTR
      DCR = DECD * DTR
      SEOD = SIN (LAR) * SIN(DCR) + COS(LAR) * COS(DCR) * COS(HAR)
      EOD = ARSIN( SEOD ) / DTR
C
      RETURN
      END
```

```
      SUBROUTINE MAGTIM(A,B,GMLT)
C THIS ROUTINE TAKES COORDINATES 'A' AND 'B' WHICH ARE RECTILINEAR
C COORDINATES IN THE MAGNETIC TIME-MAGNETIC COLATITUDE SYSTEM.THE ROUTINE
C THEN GIVES AN OUTPUT PARAMETER  'GMLT' WHICH IS MAGNETIC TIME OF THE
C OBSERVATION POINT IN THE INERTIAL  PROBLEM FRAME OF REFERENCE MENTIONED .
      PI = 3.141592654
      TPI = 6.283185308
      IF(A.NE.0.)GO TO 826
      IF(B.GT.0.)GO TO 827
      GMLT = -PI*0.5
      GO TO 828
  827 GMLT = PI*0.5
      GO TO 828
  826 GMLT = ATAN(B/A)
      IF(A.GT.0.)GO TO 828
      IF(B.LT.0.)GO TO 836
      GMLT = PI + GMLT
      GO TO 828
  836 CONTINUE
      GMLT=PI + GMLT
      GO TO 829
  828 CONTINUE
      IF(B.GE.0.)GO TO 829
      GMLT = (2.*PI) + GMLT
  829 CONTINUE
      GMLT = GMLT + (PI*0.5)
      IF(GMLT.GE.6.283)GMLT=GMLT-TPI
      RETURN
      END
```

```
      SUBROUTINE SDARD(A,B,STAND)
C THIS ROUTINE HAS INPUT OF COORDINATE (A,B),
C                  OUTPUT IS STAND . THIS IS THE VALUE OF THE STREAM FUNCTION
C                           THAT IS TRACKED BY ROUTINE 'SLINE'
C THIS ROUTINE TAKES PSI1 AND PSI2 FROM THE COMMON BLOCK AND MAKES AN ADJUSTMENT
C FOR PSI DEPENDING ON THE LOCATION OF RRR.ACTUALLY ONLY CHANGES PSI1 SO THAT
C 'SLINE' ROUTINE WILL TRACK THE STREAMLINE....(ALSO CHANGES PSI2)
      COMPLEX P1,P2,P3,P4,P5,P6,P7,P8,P9,PO,PA,PB,PC,PD,PE,PF,PG,PH,
     *Z1,Z2,Z3,Z4,Z5,Z6,Z7,Z8,Z9,ZO,ZA,ZB,ZC,ZD,ZE,ZF,ZG,ZH,ZI,IG,VELOC,
     *PL,PI,ZL,ZJ
      COMMON S,D,K1,K2,K3,K4,K5,K6,K7,K8,K9,KO,KA,KB,KC,KD,KE,KF,KG,KH,
     *W,OFFSET,STEPP,PI,
     *P1,P2,P3,P4,P5,P6,P7,P8,P9,PO,PA,PB,PC,PD,PE,PF,PG,PH,IG,
     *RK1,RK2,RK3,RK4,RK5,RK6,RK7,RK8,RK9,RKO,RKA,RKB,RKC,RKD,RKE,RKF,
     *RKG,RKH,
     *SCALE,OD,AFAC,EFAC,
     *PSI1,PSI2,PSI1IN,PSI2IN,Q1,Q2,Q3,Q4,V,VX,RRR,
     *WMIDL,LFLAG,MFLAG,
     *RKL,RKJ,KL,KJ,PL,PJ
C
C     XXX = PSI1IN
C     IF(V.EQ.1.0)GO TO 850
C     PSI1IN = XXX*0.75
C     IF(V.EQ.2.0)GO TO 850
C     PSI1IN = XXX*0.50
C     IF(V.EQ.3.0)GO TO 850
C     PSI1IN = XXX*0.20
C     IF(V.EQ.4.0)GO TO 850
C     PSI1IN = 0.0
  850 CONTINUE
      IF(VX.NE.V)PSI1IN = PSI1
      IF(VX.NE.V)PSI2IN = PSI2
      STAND = ABS(PSI1IN + PSI2IN)
C     WRITE(3,851)V,VXX,PSI1IN,PSI2IN
C 851 FORMAT(1H ,'V=',E16.5,'XXX=',E16.5,'PSI1IN=',E16.5,'PSI2IN',E16.5)
C     PSI1I; = XXX
      RETURN
      END
```

```
      SUBROUTINE FLOW(A,B,PSI)
C
C THIS ROUTIN  SOLVES  THE PLASMA FLOW PROBLEM. . IT DOES THIS BY  SOLVING
C FOR THE POTENTIAL OF TEN LINE CHARGES AND THEIR IMAGES IN A CYLINDER.
C THE  EXACT GEOMETRY  IS SHOWN IN THE THESIS.
C THE ROUTINE COMPUTES  THE STREAMFUNCTION 'PSI' AT A POINT (A,B)....
C P1---PO,PA---PJ ARE THE LOCATIONS OF THE LINE CHARGES IN THE COMPLEX PLANE.
C
      COMPLEX P1,P2,P3,P4,P5,P6,P7,P8,P9,PO,PA,PB,PC,PD,PE,PF,PG,PH,
     +Z1,Z2,Z3,Z4,Z5,Z6,Z7,Z8,Z9,ZO,ZA,ZB,ZC,ZD,ZE,ZF,ZG,ZH,ZI,ZG,VELOC,
     +PL,PJ,ZL,ZJ
      COMMON S,D,K1,K2,K3,K4,K5,K6,K7,K8,K9,KO,KA,KB,KC,KD,KE,KF,KG,KH,
     +W,OFFSET,STEPP,PI,
     +P1,P2,P3,P4,P5,P6,P7,P8,P9,PO,PA,PB,PC,PD,PE,PF,PG,PH,IG,
     +RK1,RK2,RK3,RK4,RK5,RK6,RK7,RK8,RK9,RKO,RKA,RKB,RKC,RKD,RKE,RKF,
     +RKG,RKH,
     +SCALE,DD,RFAC,EFAC,
     +PSI1,PSI2,PSI1IN,PSI2IN,Q1,Q2,Q3,Q4,V,VX,RRR,
     +WIDL,LFLAG,MFLAG,
     +RKL,RKJ,KL,KJ,PL,PJ
C     XXX     'W' IS ANGULAR VELOCITY OF EARTH   XXXXXXXXXXXXXXXXXXXXXX
C
      Z = CMPLX(A,B)
      Z1 = Z - P1
      Z2 = Z - P2
      Z3 = Z - P3
      Z4 = Z - P4
      Z5 = Z - P5
      Z6 = Z - P6
      Z7 = Z - P7
      Z8 = Z - P8
      Z9 = Z - P9
      ZO = Z - PO
      ZA = Z - PA
      ZB = Z - PB
      ZC = Z - PC
      ZD = Z - PD
      ZE = Z - PE
      ZF = Z - PF
      ZG = Z - PG
      ZH = Z - PH
      ZL = Z - PL
      ZJ = Z - PJ
      R1 = CABS(Z1)
      R2 = CABS(Z2)
      R3 = CABS(Z3)
      R4 = CABS(Z4)
      R5 = CABS(Z5)
      R6 = CABS(Z6)
      R7 = CABS(Z7)
      R8 = CABS(Z8)
      R9 = CABS(Z9)
      RO = CABS(ZO)
      RA = CABS(ZA)
      RB = CABS(ZB)
      RC = CABS(ZC)
      RD = CABS(ZD)
      RE = CABS(ZE)
      RF = CABS(ZF)
```

```
      RG = CABS(ZG)
      RH = CABS(ZH)
      RL = CABS(ZL)
      RJ = CABS(ZJ)
      PSI = RK1 * ALOG(R1)
     ** RK2 * ALOG(R2)
     ** RK3 * ALOG(R3)
     ** RK4 * ALOG(R4)
     ** RK5 * ALOG(R5)
     ** RK6 * ALOG(R6)
     ** RK7 * ALOG(R7)
     ** RK8 * ALOG(R8)
     ** RK9 * ALOG(R9)
     ** RKO * ALOG(RO)
     ** RKA * ALOG(RA)
     ** RKB * ALOG(RB)
     ** RKC * ALOG(RC)
     ** RKD * ALOG(RD)
     ** RKE * ALOG(RE)
     ** RKF * ALOG(RF)
     ** RKG * ALOG(RG)
     ** RKH * ALOG(RH)
     ** RKL * ALOG(RL)
     ** RKJ * ALOG(RJ)
      PSI1 = PSI
      COLAT = (RRR * SCALE)/111.
      COLAT = (COLAT * PI)/180.
      ADJUST = (6360. * (COLAT - SIN(COLAT) ) )/SCALE
      RRRR = RRR - ADJUST
      PSI2 = 0.5 * W*RRRR * RRRR
      PSI = PSI1 + PSI2

      PSI EQUAL CONSTANT DEFINES A STREAMLINE **************************
      WRITE(3,69)PSI1,PSI2,RKA,RKB,RRR,RRRR
   69 FORMAT(1H ,'PSI1=',E16.5,'   PSI2=',E16.5,'   RKA=',E16.5,
     *'   RKB=',E16.5,'   RRR=',E16.5,'   RRRR=',E16.5)

      RETURN
      END
```

```
      SUBROUTINE FOTOIZ(QO,CHI,SIGMA,MODEL,Z,QCHI)
C
C THIS ROUTINE IS CALLED BY ROUTINE 'SOLAR'.
C THIS ROUTINE 'FOTOIZ' CALCULATES 'QCHI' THE PHOTO-IONIZATION RATE FOR SOLAR
C ZENITH ANGLE  'CHI'.....
C  OTHER PARAMETERS ARE DEFINED IN 'SOLAR'....
C
      REAL K,L,M,LOCHI,MODEL(36,3)
      PI2=1.5708
      RE=6360.
C
      FXO = 1.0
C
      IZ=1
C
C     WRITE(3,7777)Z
C7777 FORMAT(1H ,'Z=',E16.5)
  774 CONTINUE
      IF(MODEL(IZ,1).EQ.Z)GO TO 775
      IZ=IZ+1
      GO TO 774
  775 CONTINUE
C     WRITE(3,772)MODEL(IZ,1)
C     WRITE(3,772)MODEL(IZ,2)
C     WRITE(3,772)MODEL(IZ,3)
      Z= MODEL(IZ,1)
      H=MODEL(IZ,2)
      DENS= MODEL(IZ,3)
      TAUO = DENS * H*100000.* SIGMA * FXO
C
C     SCALE HEIGHT IN KILOMETRES
C
      L=((RE+Z)*( COS(CHI-PI2)))-RE
C     WRITE(3,772)L
      X=(RE+Z)/H
C     WRITE (3,772)X
      Y=(RE+L)/H
C     WRITE (3,772) Y
C
C
      IF(CHI.GE.PI2) GO TO 770
      AT=ALOG (( PI2*X) ** 0.5 )
C     WRITE (3,772) AT
      BT = 1.234 / AT
C     WRITE (3,772) BT
      ALPHA = ( 0.7162 - BT )/ 6.088
C     WRITE (3,772) ALPHA
      CT = 0.5 * CHI*CHI
C     WRITE (3,772) CT
      DT = (1.0) - ( 0.115 * CHI * CHI ) -(ALPHA*CHI*CHI*CHI*CHI)
C     WRITE (3,772) DT
      FXCHI = EXP( CT/DT )
      TAUCHI = DENS * H*100000. * SIGMA * FXCHI
      TAUDIF=TAUO - TAUCHI
C
      GO TO 771
C
  770 CONTINUE
C
```

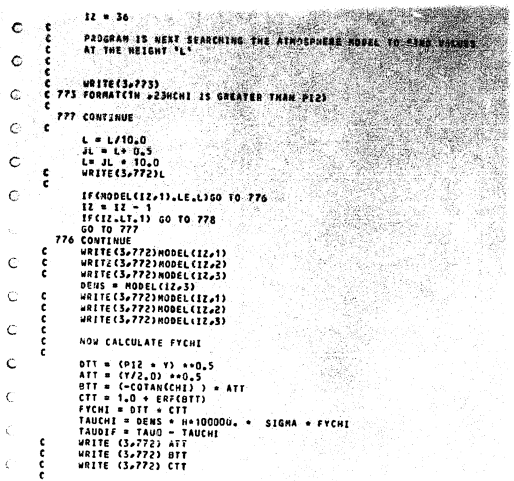

```
      IZ = 36
C     
C     PROGRAM IS NEXT SEARCHING THE ATMOSPHERE MODEL TO FIND VOLUME
C     AT THE HEIGHT 'L'
C     
C     
C     WRITE(3,773)
C 773 FORMAT(1H ,23HCHI IS GREATER THAN PI/2)
C     
  777 CONTINUE
C     
      L = L/10.0
      JL = L+ 0.5
      L= JL * 10.0
C     WRITE(3,772)L
C     
      IF(MODEL(IZ,1).LE.L)GO TO 776
      IZ = IZ - 1
      IF(IZ.LT.1) GO TO 778
      GO TO 777
  776 CONTINUE
C     WRITE(3,772)MODEL(IZ,1)
C     WRITE(3,772)MODEL(IZ,2)
C     WRITE(3,772)MODEL(IZ,3)
      DENS = MODEL(IZ,3)
C     WRITE(3,772)MODEL(IZ,1)
C     WRITE(3,772)MODEL(IZ,2)
C     WRITE(3,772)MODEL(IZ,3)
C     
C     NOW CALCULATE FYCHI
C     
      DTT = (PI2 * Y) **0.5
      ATT = (Y/2.0) **0.5
      BTT = (-COTAN(CHI) ) * ATT
      CTT = 1.0 + ERF(BTT)
      FYCHI = DTT * CTT
      TAUCHI = DENS * H*100000. *  SIGMA * FYCHI
      TAUDIF = TAUO - TAUCHI
C     WRITE (3,772) ATT
C     WRITE (3,772) BTT
C     WRITE (3,772) CTT
C     
  771 CONTINUE
C     
C     WRITE (3,772) FXCHI
C     WRITE (3,772) FXO
C 772 FORMAT (1H ,E16.5)
      LQCHI=(ALOG(QO)) +( TAUDIF )
C     
C     HAVE MUTIPLIED H BY 100000. TO BRING UNITS BACK TO CMS
      QCHI = EXP(LQCHI)
  780 CONTINUE
C     WRITE (3,772) QCHI
      RETURN
  778 CONTINUE
C     WRITE(3,779)
C 779 FORMAT(1H ,30HSOLAR DEPRESSION ANGLE TOO LOW)
      QCHI = 0.0
      GO TO 780
      END
```

```
      SUBROUTINE SOLAR(A,B,IDAY,UTFIX,UTIT,AINV,GLON,
     *GST,RA,DC,EOD,PI,SCALE,
     *QO,CHI,SIGMA,MODEL,Z,QCHI)
C THIS ROUTINE COMPUTES THE SOLAR PHOTO IONIZATION RATE (I.E. ELECTRON DENSITY)
C IT IS ACTUALLY FOTOIZ THAT. THAT WOULD BE MAIN ENTRY AND ALL OF THE ROUTINE
C DOES THE REVELANT TRANSFORMATIONS TO THE SOLAR-FIXED COORDINATES.
C
C INPUTS-------A,B = COORDINATES OF POINT
C              IDAY = DAY OF YEAR (D----360)
C                     UTFIX = UNIVERSAL TIME IN H*CHOS AT WHICH ONE WISHES TO WORK
C                             THE PROBLEM.
C                     UTIT= ADUMMY VARIABLE NO LONGER USED IN FINAL PROGRAM.
C                     AINV=AN ARRAY NEEDED BY ROUTINE 'INTERP'
C                          (SEE 'INTERP' FOR DETAILS.
C                     WIND= A VARIABLE NO LONGER USED IN FINAL PROGRAM.
C                     GST,RA,DC,EOD,= VARIABLES REQUIRED BY ROUTINE 'ELDEP'.
C                     PI = 3.14-------
C                     SCALE = CONVERSION FACTOR PROBLEM UNITS TO KILOMETRES.
C                     QO,CHI,SIGMA,RCHI= VAIABLES USED BY ROUTINE FOTOIZ.
C                     Z = ALTITUDE IN KILOMETRES.
C                     MODEL= ATMOSPHERIC MODEL READ IN FROM CARDS AT BEGINNING OF
C                            MAIN PROGRAM.
C OUTPUT IS 'QCHI'-----THIS IS PHOTO IONIZATION RATE FOR SOLAR ZENITH ANGLE CHI.
C
      REAL LAT,LONG
      REAL INLAT,INLON
      REAL N2,NE,INT
      REAL MODEL(36,5)
      DIMENSION UT(3),GST(3),RA(4),DC(4)
      DIMENSION AINV(72,10)
      EQUIVALENCE (LAT,GLAT),(LONG,GLON)
C
      PI2 = 1.5708
      RRRR = A*A + B*B
      RRR = SQRT(RRRR)
      COLAT = RRRR * SCALE / 111.0
      INLAT = 90. - COLAT
      UTT = UTFIX
C     WRITE(3,5)A,B,RRRR,COLAT,INLAT
C  5  FORMAT(1H ,'A=',F5.2,' B=',F5.2,' RRRR=',F5.2,' COLAT=',E16.5,'
C     *INLAT=',E16.5)
      CALL MAGTIM(A,B,GMLT)
      CALL MINLON(GMLT,UTT,IDAY,INLON)
      INLON = (INLON * 180.)/PI
C     WRITE(3,6)GMLT,INLON
C  6  FORMAT(1H ,'GMLT=',E16.5,' INLON=',E16.5)
      CALL INTERP(INLAT,INLON,GLAT,GLON,AINV)
C     WRITE(3,9)UTT
C  9  FORMAT(1H ,'UTIT=',E16.5)
      JUTT = UTT/3600.
      UT(1) = JUTT
      AUTT =  UTT -(UT(1) * 3600.)
      JUTT = AUTTT / 60.
      UT(2) = JUTTT
      AUTTT = UTTT - ( (UT(1) * 3600.) + ( UT(2) * 60.) )
      UT(3) = AUTTT
      CALL = ELDEP(LAT,LONG,UT,GST,RA,DC,EOD)
C     WRITE(3,8)LAT,LONG,UT,GST,RA,DC,EOD
C  8  FORMAT(1H ,'ELDEP ',17F7.1)
      CHI = PI2 - EOD*PI2/90.0)
C     WRITE(3,7)CHI,EOD,U
C  7  FORMAT(1H ,'SOLAR STUFF IS',5E16.5)
      CALL FOTOIZ(QO,CHI,SIGMA,MODEL,Z,QCHI)
      RETURN
      END
```

```
      COLAT = (COLAT + PI)/180.
      ADJUST = (6360. + (COLAT - SIN(COLAT) ) )/SCALE
      CVR = -W*(COLAT - ADJUST)
      CVI = CVR * COS(THETA)
      CVR = -CVR * SIN(THETA)
      VR = VR + CVR
      VI = VI + CVI
      VELOC = CMPLX(VR,VI)
C     XXXXXXXXXXXXXXXXXXXXXXXXXXXXXXXXXXXXXXXXXXXXXXXXXXXXXXXXXXXXXXXXXXXXXXXXXXXXXXX
C     -
      DELTA = 1.570796327
      IF(VR.EQ.0.)GO TO 18
      DELTA = ATAN(VI/VR)
      IF(VR.GT.0.)GO TO 20
   18 CONTINUE
      IF(VI.LT.0.)GO TO 19
      DELTA = PI - ABS(DELTA)
      GO TO 20
   19 CONTINUE
      DELTA = -PI + ABS(DELTA)
   20 CONTINUE
      DIREC = DELTA
C     XXXXXXXXXXXXXXXXXXXXXXXXXXXXXXXXXXXXXXXXXXXXXXXXXXXXXXXXXXXXXXXXXXXXXXXXXXXXXXX
      SPEED = CABS(VELOC)
C
   10 CONTINUE
      RETURN
      END
```

```
      SUBROUTINE CLOSS(N2,O2,NE,INT,CL,BETA)
      REAL N2,NE,INT
C     XXXXXXXXXXXXXXXXXXXXXXXXXXXXXXXXXXXXXXXXXXXXXXXXXXXXXXXXXXXXXXXX
C     XXX   GIVEN 'O2','N2' NEUTRAL NUMBER DENSITIES,'NE' ELECTRON      XXX
C     XXX   DENSITIY ,AND TIME INTERVAL 'INT' SECONDS,                  XXX
C     XXX   THIS SUBROUTINE COMPUTES THE IONIZATION LOSS 'CL',          XXX
C     XXX   DUE TO CHEMICAL RECOMBINATION.                              XXX
C       IT ALSO COMPUTES  BETA THE ELECTRON LOSS RATE....
C     XXXXXXXXXXXXXXXXXXXXXXXXXXXXXXXXXXXXXXXXXXXXXXXXXXXXXXXXXXXXXXXX
      IF(NE.LE.0.0)NE = 0.00001
      ALPHA2 = 7.99 E-08
      ALPHA5 = 1.88 E-07
      RATE3 = 1.39 E-12
      RATE4 = 7.21 E-12
      BETA = (RATE3 * N2) + (RATE4 * O2 )
      DASH = 1. + ( (RATE4*O2)/(ALPHA2*NE))+((RATE3*N2)/(ALPHA5*NE) )
      BETA = BETA / DASH
      Q = BETA * NE
      CL = INT * Q
C     WRITE(3,5)INT,BETA,CL
C   5 FORMAT(1H ,20HTIME INTERVAL(SECS)=,F8.1,5HBETA=,E16.5,
C    110HCHEM LOSS=,E16.5)
      RETURN
      END
```

```
      SUBROUTINE FLUX(OP200,OP250,OP300,OP350,OP400,AINC,WIND,DELT)
C THIS ROUTINE COMPUTES DIFFUSION VELOCITIES AND FLUX ACROSS LEVELS 200 TO 400
      OP500 = 0.329 * OP300
      FYSTA = (1.0 E+03) * OP500
C
      OP225 = (OP200 + OP250 )/2.0
      OP175 = 2.0*OP200 - OP225
      OP275 = (OP250 + OP300)/2.0
      OP325 = (OP300 + OP350)/2.0
      OP375 = (OP350 + OP400)/2.0
      OP425 = ( (OP400-OP300)/4.0 ) + OP400
      IF(OP175.LT.0.0) OP175=0.0
      IF(OP425.LT.0.0)OP425=0.0
C
C
      TA =((OP175 + OP200)*(2.5 E+06) )/2.0
     * + ((OP200+OP225)*(2.5 E+06))/2.0
     * + ((OP225+OP275)*(5.0 E+06))/2.0
     * + ((OP275+OP325)*(5.0 E+06))/2.0
     * + ((OP325+OP375)*(5.0 E+06))/2.0
     * + ((OP375+OP425)*(5.0 E+06))/2.0
C
      IF(TA.LE.0.)GO TO 91
C
C
      TCC = DELT * FYSTA
      ZZ = (TA - TCC)/TA
      OP200 = OP200 * ZZ
      OP250 = OP250 * ZZ
      OP300 = OP300 * ZZ
      OP350 = OP350 * ZZ
      OP400 = OP400 * ZZ
C
   91 CONTINUE
C
C     WRITE(3,90)ZZ,OP200,OP250,OP300,OP350,OP400
C  90 FORMAT(1H ,'ZZ=',E16.5,2X,5E16.5)
C
      IF(OP200.LT.0.0)OP200=0.0
      IF(OP250.LT.0.0)OP250=0.0
      IF(OP300.LT.0.0)OP300=0.0
      IF(OP350.LT.0.0)OP350=0.0
      IF(OP400.LT.0.0)OP400=0.0
C
      RETURN
      END
```

```
      SUBROUTINE CAR(A,B,KK)
C
C INPUT-------A&B=COORDINATES OF A POSITION IN THE COMPLEX PLANE
C                 A ALONG X-AXIS, B ALONG THE Y-AXIS.
C OUTPUT-KK - THIS IS THE VORTICITY FACTOR THAT DEFINES THE SPEED OF PLASMA FLOW
C
      REAL KK,K1,K2,K3,K4,K5,K6,K7,K8,K9,KO,P1,K10,K11,K12,K13,K14,K15,K16,K17,
     *K18
      COMPLEX P1,P2,P3,P4,P5,P6,P7,P8,P9,PO,PA,PB,PC,PD,PE,PF,PG,PH,
     *Z1,Z2,Z3,Z4,Z5,Z6,Z7,Z8,Z9,ZO,ZA,ZB,ZC,ZD,ZE,ZF,ZG,ZH,ZI,VELOC,
     *PL,PJ,ZL,Z3
      COMMON S,DX,K1,K2,K3,K4,K5,K6,K7,K8,K9,KO,KA,KB,KC,KD,KE,KF,KG,KH,
     *W,OFFSET,STEPP,P1,
     *P1,P2,P3,P4,P5,P6,P7,P8,P9,PO,PA,PB,PC,PD,PE,PF,PG,PH,ZO,
     *RK1,RK2,RK3,RK4,RK5,RK6,RK7,RK8,RK9,RKO,RKA,RKB,RKC,RKD,RKE,RKF,
     *RKG,RKH,
     *SCALE,DD,RFAC,EFAC,
     *PSI1,PSI2,PSI1IN,PSI2IN,Q1,Q2,Q3,Q4,V,VX,RRR,
     *WNIDL,LFLAG,NFLAG,
     *RKL,RKJ,KL,KJ,PL,PJ
      VX = V
      RKK = KK
      RRR = AAA + (B+OFFSET)*(B+OFFSET)
      RRR = SQRT(RRR)
C
      QL1 = 0.78
      QL2 = 0.55
      QL3 = 0.33
      QL4 = 0.11
      QR1 = 1.2
      QR2 = 1.4
      QR3 = 1.6
      QR4 = 1.8
      IF(LFLAG.NE.2)GO TO 500
      QL1 = 1.2
      QL2 = 1.4
      QL3 = 1.6
      QL4 = 1.8
      QR1 = 0.78
      QR2 = 0.55
      QR3 = 0.33
      QR4 = 0.11
  500 CONTINUE
C
C
      V = 1.
      IF(RRR.LE.Q1) GO TO 637
      V = 2.
      IF(RRR.LE.Q2) GO TO 638
      V = 3.
      IF(RRR.LE.Q3) GO TO 639
      V = 4.
      IF(RRR.LE.Q4) GO TO 640
      V = 5.
      KK = 0.0
      GO TO 637
  638 KK = KK + 0.75
      GO TO 637
  639 KK = KK + 0.50
```

```
      GO TO 637
  640 KK = KK + 0.20
      GO TO 637
  641 KK = KK+0.10
  637 CONTINUE
      EFAC = 1.0
      RFAC = 1.0
      IF(CLFLAG.EQ.0)GO TO 642
      IF(CRR.GE.1.3)GO TO 642
      V = -1.0
      IF(A.GT.-0.3.AND.A.LT.+0.3)GO TO 642
      V = -2.0
      IF(A.LE.-0.3.AND.A.GT.-0.6)GO TO 643
      IF(A.GE.+0.3.AND.A.LT.+0.6)GO TO 644
      V = -3.0
      IF(A.LE.-0.6.AND.A.GT.-0.9)GO TO 645
      IF(A.GE.+0.6.AND.A.LT.+0.9)GO TO 646
      V = -4.0
      IF(A.LE.-0.9.AND.A.GT.-1.3)GO TO 647
      IF(A.GE.+0.9.AND.A.LT.+1.3)GO TO 648
      CONTINUE
  643 KK = KK + QL1
      GO TO 642
  644 KK = KK + QR1
      GO TO 642
  645 KK = KK + QL2
      GO TO 642
  646 KK = KK + QR2
      GO TO 642
  647 KK = KK + QL3
      GO TO 642
  648 KK = KK+ QR3
  642 CONTINUE
      K1 = KK + EFAC
      K3 = KK + EFAC
      K5 = KK + EFAC
      K8 = KK + RFAC
      K9 = KK + RFAC
      KF = KK + RFAC
      K2 =-KK + RFAC
      K4 =-KK + RFAC
      K6 =-KK + RFAC
      KA =-KK + EFAC
      KC =-KK + EFAC
      KE =-KK + EFAC
      K7 = +KK+ EFAC
      K8 = -KK+ RFAC
      K9 = +KK+ EFAC
      KQ = -KK+ RFAC
      KG = -KK+ EFAC
      KH = +KK+ RFAC
      KL = -KK+ EFAC
      RK2 = K2
      KJ = +KK+ RFAC
      RK1 = K1
      RK3 = K3
      RK4 = K4
      RK5 = K5
      RK6 = K6
      RK7 = K7
```

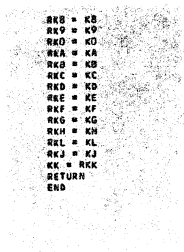

```
RK8 = K8
RK9 = K9
RKO = KO
RKA = KA
RKB = KB
RKC = KC
RKD = KD
RKE = KE
RKF = KF
RKG = KG
RKH = KH
RKL = KL
RKJ = KJ
KK = RKK
RETURN
END
```

```
      SUBROUTINE MINLON(GMLT,UXT,IDAY,INLON)
C THIS ROUTINE COMPUTES  THE MAGNETIC LONGITUDE  OF THE OBSERVATION POINT
C 'INLON'.  INPUTS ARE MAGNETIC LOCAL TIME,UNIVERSAL TIME(IN SECONDS),DAY OF YEAR
C ---CODE MAKES  SLIGHT CORRECTION TO'UT' TO ALLOW FOR FOR SEASONAL CHANGE
C IN THE TRANSFORMATION FROM  UT TO MAGNETIC TIME.
C UT IN SECONDS,GMLT IN RADIANS,,INLON IN RADIANS TOO.
C
      REAL INLON
      S1 = 0.438356
C 'S1' IS 80./182.5
C
      IF(IDAY.GT.182)GO TO 10
      DAY = IDAY
      CORR = (S1* DAY)-40.
      GO TO 11
   10 CONTINUE
      DAY = IDAY
      CORR = (-S1 *( DAY-182.))+40.
   11 CONTINUE
      CORR = CORR*60.
      UTT = UTT + CORR
      IF(UTT.LT.0.)UTT = UTT+86400.
C THE FACTOR '7.2722 E-05' IS CONVERSION OF SECONDS TIME TO RADIANS ANGLE.
      UTT= UTT* (7.2722 E-05)
C THE CONSTANT '1.1868' IS THE ANGLE IN RADIANS BETWEEN THE UT MERIDIAN AND
C THE THE  GEOMAGNETIC ZERO MERIDIAN.........
      INLON = GMLT - UTT + 1.1868
      IF(INLON.GE.6.283185)INLON=INLON-6.283185
      IF(INLON.LT.0.)INLON=INLON+6.283185
      UTT= UTT/ (7.2722 E-05)
      RETURN
      END
```

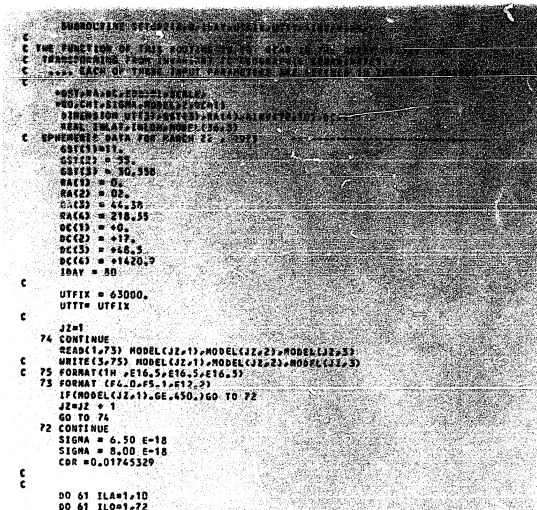

```
      SUBROUTINE SET_UP(AINV,MODEL,UTFIX,IDAY)
C
C THE FUNCTION OF THIS ROUTINE IS TO CLEAR OUT THE ARRAY
C TRANSFORMING FROM INVARIANT TO GEOGRAPHIC LATITUDES,
C ... EACH OF THESE INPUT PARAMETERS ARE LISTED IN THE
C
      REAL*4 AINV(72,10),
     *MODEL(72,3),UTFIX
      DIMENSION UT(3),GST(3),RA(3),DEC(3),
      REAL IMLAT,IMLONG,MODEL(36,3)
C  EPHEMERIS DATA FOR MARCH 22 , 1971
      UT(1)=21.
      UT(2) = 22.
      UT(3) = 50.550
      RA(1) = 0.
      RA(2) = 02.
      RA(3) = 22.35
      RA(4) = 218.55
      DEC(1) = +0.
      DEC(2) = +17.
      DEC(3) = +48.5
      DEC(4) = +1420.9
      IDAY = 80
C
      UTFIX = 63000.
      UTTT= UTFIX
C
      JZ=1
   74 CONTINUE
      READ(1,73) MODEL(JZ,1),MODEL(JZ,2),MODEL(JZ,3)
C     WRITE(3,75) MODEL(JZ,1),MODEL(JZ,2),MODEL(JZ,3)
C  75 FORMAT(1H ,E16.5,E16.5,E16.5)
   73 FORMAT (F4.0,F5.1,E12.2)
      IF(MODEL(JZ,1).GE.450.)GO TO 72
      JZ=JZ + 1
      GO TO 74
   72 CONTINUE
      SIGMA = 6.50 E-18
      SIGMA = 8.00 E-18
      CDR =0.01745329
C
C
      DO 61 ILA=1,10
      DO 61 ILO=1,72
      READ(1,60)AINV(ILO,ILA)
   60 FORMAT(F7.2)
   61 CONTINUE
C     XXX    ABOVE READ IN AINV ARRAY(INVARIANT LATITUDE V/S
C     XXX   GEOGRAPHIC LATITUDE.   XXXXXXXXXXXXXXXXXXXXXXXXXXXXXXXXXX
      DO 63 ILA=1,10
C     WRITE(3,64)
C  64 FORMAT(1H1)
      DO 63 ILO=1,72
C     WRITE(3,62)AINV(ILO,ILA)
C  62 FORMAT(1H ,F7.2)
   63 CONTINUE
C     XXX   ABOVE PRINT OUT AINV ARRAY FOR CHECKING XXXXXXXXXXXXXXXXXXX
C     WRITE(3,65)
C  65 FORMAT(1H1,10X,24HRESULTS OF INTERPOLATION)
      RETURN
      END
```

```
      SUBROUTINE INPROF(OP200,OP250,OP300,OP350,OP400,R1)
C
C  THIS  ROUTINE SETS THE INITIAL DENSITY PROFILE VALUES AT 200---400KM
C ALTITUDES.
C THE VALUES  HERE ARE ONLY SAMPLES ..
C    IN PRACTICE
C   IN PRACTICE THE  VALUES  MUST BE ARRIVED AT BY  FIRST RUNNING THE PROGRAM
C ONCE AROUND THE STREAMLINE...
C
      OP200 = 0.897 E+05
      OP250 = 0.243 E+06
      OP300 = 0.363 E+06
      OP350 = 0.275 E+06
      OP400 = 0.208 E+06
      RETURN
      END
```

```
      SUBROUTINE INTERP(INLAT,INLON,GLAT,GLON,AINV)
C
C INPUTS--  INLAT= INV LATITUDE
C           INLON = INV LONGITUDE
C           AINV IS AN ARRAY OF GEOG. LATITUDES  AND LONGITUDES
C           CORRESPONDING TO INV. LATS AND LONGS.
C OUTPUTS-- GLON= GEOGRAPHIC LONGITUDE
C           GLAT= GEOG. LATITUDE
C-------------GIVEN THE GEOG LATS AND LONGITUDES THE ROUTINE
C              FOLLOWS A FOUR POINT INTERPOLATION WITHIN THE *AINV* ARRAY TO
C              GET A GEOGRAPHIC LAT AND LONG----------------------------
C
      DIMENSION AINV(72,10)
      REAL INLAT,INLON
      ILO = INLON / 10.
      ILO = (2* ILO) + 1
   30 CONTINUE
      IF(ILO.LE.72) GO TO 31
      ILO = ILO - 72
      GO TO 30
   31 CONTINUE
      ILOO = ILO + 2
   32 CONTINUE
      IF(ILOO.LE.72)GO TO 33
      ILOO  = ILOO - 72
      GO TO 32
   33 CONTINUE
      RILA = (90. - INLAT)/ 5.0
      ILA = RILA
      ILA = ILA + 1
      RINLAT = 90. - (5. * (ILA - 1) )
      RINLON = (ILO/2) * 10.
C
C     XXX NEXT HAVE TWO SETS
C     XXX OF    FOUR POINTS,      GLA1  GLA2      GLO1  GLO2
C     XXX G/LAT SET AND
C     XXX G/LONGITUDE SET --      GLA3  GLA4      GLO3  GLO4
C     XXX THEN WISH TO INTER-
C     XXX POLATE BETWEEN THESE
C     XXX FOUR POINTS FOR
C     XXX EACH SET.............
      GLA1 = AINV(ILO,ILA)
      GLA2 = AINV(ILOO,ILA)
      GLA3 = AINV(ILO,ILA+1)
      GLA4 = AINV(ILOO,ILA+1)
C
      GLO1 = AINV(ILO+1,ILA)
      GLO2 = AINV(ILOO+1,ILA)
      GLO3 = AINV(ILO+1,ILA+1)
      GLO4 = AINV(ILOO+1,ILA+1)
C
      G1 = ABS( GLO1 - GLO3 )
      IF(G1.LE.180.)GO TO 20
      GA = GLO1
      IF(GLO1.GT.GLO2)GLO1 = GLO1 - 360.
      IF(GLO2.GT.GA)GLO2=GLO2 - 360.
   20 CONTINUE
      G2 = ABS(GLO2 - GLO4)
      IF(G2.LE.180.)GO TO 21
```

```
      GB = GL02
      IF(GL02.GT.GL04)GL02=GL02 - 360.
      IF(GL04.GT.GB) GL04 = GL04 - 360.
   21 CONTINUE
C
C     XXX NEXT DO THE INTERPOLATION
      GLATA=-(((GLA1-GLA3)/5.)* (RINLAT - INLAT) ) + GLA1
      GLATB=-(((GLA2-GLA4)/5.)* (RINLAT - INLAT) ) + GLA2
      GLONA=-(((GL01-GL03)/5.)* (RINLAT - INLAT) ) + GL01
      GLONB=-(((GL02-GL04)/5.)* (RINLAT - INLAT) ) + GL02
      GLAT =-( ( (GLATA-GLATB)/10.)*(ABS(RINLON-INLON) ) ) + GLATA
C
      G3 = ABS( ABS(GLONA) - ABS(GLONB) )
      IF(G3.LT.180.)GO TO 22
      GC = GLONA
      IF(GLONA.GT.GLONB)GLONA=GLONA - 360.
      IF(GLONB.GT.GC)GLONB = GLONB - 360.
   22 CONTINUE
C
      GLON =-( ( (GLONA-GLONB)/10. )* ( ABS(RINLON-INLON) ) ) + GLONA
      IF(GLON.LT.0.)GLON = GLON + 360.
C     WRITE(3,34)ILO,ILOO,ILA
C  34 FORMAT(1H1,4HILO=,I4,2X,5HILOO=,I4,2X,4HILA=,I4)
C     WRITE(3,35)GLAT,GLA2,GLA3,GLA4
C  35 FORMAT(1H ,12HGLA1 TO GLA4,2X,4F10.2)
C     WRITE(3,36)GL01,GL02,GL03,GL04
C  36 FORMAT(1H ,12HGL01 TO GL04,2X,4F10.2)
C     WRITE(3,37)GLATA,GLATB,GLONA,GLONB
C  37 FORMAT(1H ,'GLATA=',E16.5,2X,'GLATB=',E16.5,2X,'GLONA=',E16.5,
C    *2X,'GLONB=',E16.5)
C     WRITE(3,38)RINLAT,RINLON
C  38 FORMAT(1H ,'RINLAT=',F8.2,2X,'RINLON=',F8.2)
C     WRITE(3,39)GLAT,GLON
C  39 FORMAT(1H ,'GLAT=',E16.5,' GLON=',E16.5)
      RETURN
      END
```

```
      SUBROUTINE AURORA(A,H,AU200,AU250,AU300,AU350,AU400)
C
C THIS ROUTINE COMPUTES THE IONIZATION RATE FROM 200 TO 400 KMS ALTITUDE
C        AT  A POINT (A,H). THESE RATES ARE AU200----AU400.  THESE ARE FOR
C        DIFFUSE AURORA(DAY AND NIGHT-SIDE AURORAL OVAL). THE RATES COME FROM
C        BANKS,CHAPPELL,AND NAGY ---JGR(1974)
C
      A1 = SQRT( A**2 + (H*0.9)*(H*0.9) )
      A2 = SQRT(A**2 + H**2)
      A3 = SQRT(A**2 + (H+0.2)*(H+0.2) )
      IF(H.LE.4.0)GO TO 15
      IF(A1.GT.1.5.AND.A1.LT.2.1)GO TO 16
      GO TO 17
   15 CONTINUE
      IF(A2.GT.1.4.AND.A3.LT.2.1)GO TO 16
C
      AU200 = 0.0
      AU250 = 0.0
      AU300 = 0.0
      AU400 = 0.0
C
   17 CONTINUE
      RETURN
   16 AU200 = 20.
      AU250 = 11.0
      AU300 = 10.
      AU350 = 7.0
      AU400 = 6.0
      RETURN
      END
```

```
      SUBROUTINE CORRT(A,B,KK,PSI,STAND,KFLAG)
C
C       THIS ROUTINE IS NO LONGER USED IN THE FINAL PROGRAM.....
C         IT IS USED FOR MAKING  A SMALL STEP CHANGE IN THE STREAMLINE AT A
C         POINT.  THIS IS ONLY  FOR  EXPERIMENTAL MODIFICATION OF STREAMLINE
C      THAT THE USER MAY  PLAY WITH..     IT CAN BE SAFELY IGNORED FOR SOLVING
C         THE PROBLEM OF THE THESIS.....
C       ALLL PARAMETERS HAVE BEEN DEFINED ELSEWHERE.....
C
       REAL KK
       COMPLEX P1,P2,P3,P4,P5,P6,P7,P8,P9,P0,PA,PB,PC,PD,PE,PF,PG,PH,
     *Z1,Z2,Z3,Z4,Z5,Z6,Z7,Z8,Z9,ZO,ZA,ZB,ZC,ZD,ZE,ZF,ZG,ZH,ZI,GVELOC,
     *PL,PJ,ZL,ZJ
       COMMON S,D,K1,K2,K3,K4,K5,K6,K7,K8,K9,KO,KA,KB,KC,KD,KE,KF,KG,KH,
     *W,OFFSET,STEPP,PI,
     *P1,P2,P3,P4,P5,P6,P7,P8,P9,P0,PA,PB,PC,PD,PE,PF,PG,PH,IG,
     *RK1,RK2,RK3,RK4,RK5,RK6,RK7,RK8,RK9,RKO,RKA,RKB,RKC,RKD,RKE,RKF,
     *RKG,RKH,
     *SCALE,ODD,RFAC,EFAC,
     *PSI1,PSI2,PSI11N,PSI2IN,Q1,Q2,Q3,Q4,VX,RRR,
     *WMIDL,LFLAG,MFLAG,
     *RKL,RKJ,KL,KJ,PL,PJ
       KFLAG=1
       B = B - 0.02
       CALL KAY(A,B,KK)
       CALL FLOW(A,B,PSI)
       STAND = ABS(PSI)
       CALL SOARD(A,B,STAND)
       RETURN
       END
```